LEVEL II

AD A103773

Technical Report	580
	M.L. Meeks
Radar Propagation at Low Altitudes: A Review and Bibliography	31 July 1981

Lincoln Laboratory

MASSACHUSETTS INSTITUTE OF TECHNOLOGY

LEXINGTON, MASSACHUSETTS

DTIC
ELECTE
SEP 4 1981
S D
A

81 9 03 009

This technical report has been reviewed and is approved for publication.

FOR THE COMMANDER
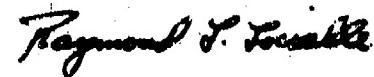
Raymond L. Loiselle, Lt.Col., USAF
Chief, ESD Lincoln Laboratory Project Office

MASSACHUSETTS INSTITUTE OF TECHNOLOGY

LINCOLN LABORATORY

RADAR PROPAGATION AT LOW ALTITUDES:
A REVIEW AND BIBLIOGRAPHY

M.L. MEEKS

Group 48

TECHNICAL REPORT 580

31 JULY 1981

LEXINGTON   MASSACHUSETTS

81 9   03 003

ABSTRACT

This report reviews the subject of electromagnetic wave propagation near the earth's surface as it relates to the detection of low-flying aircraft by ground-based radars. Separate sections describe how current knowledge of the three fundamental physical phenomena -- refraction, reflection, and diffraction -- is applied to the problems of low-altitude propagation. Simple models incorporating these phenomena are discussed: (1) propagation over a plane with arbitrary reflection coefficient, (2) propagation over a knife-edge on a plane, and (3) propagation over a smooth, spherical earth. Computer programs for models (2) and (3) are given in the Appendices. We include a bibliography of the literature on which this report is based: books, journal articles, and technical reports. References are listed alphabetically by first author, and subject indices are given for major subject headings.

iii

CONTENTS

CONTENTS (Continued)

LIST OF ILLUSTRATIONS

LIST OF ILLUSTRATIONS (Continued)

LIST OF TABLES

viii

1. INTRODUCTION

This report is intended as a tutorial review of the physics of radio propagation at low altitudes over various kinds of terrain. The objective here is to bring together an account of what is known about the propagation effects that determine the performance of ground-based radars against aircraft targets flying at low altitudes.

The propagation of electromagnetic waves has been studied actively for over 50 years with a number of objectives. These include telecommunication and television coverage prediction, microwave-link design, studies of mobile radar communication, and radar performance and design studies. We have reviewed the literature in these fields, and we include here a bibliography referencing, in separate sections, books, journal articles, and technical reports on this subject. Document references in the bibliography are listed alphabetically by the names of the first-listed author; journal articles and reports are additionally indexed by subject. References cited in the text distinguish between books, journal articles, and technical reports. For books the authors' names appear in capital letters; for example BORN & WOLF (1959). For journal articles only the first letters of the authors' names are capitalized; for example, Day and Trolese (1950). Finally, for technical reports the capital letter R appears before the year designation; for example, Longley and Rice (R 1968). Papers that have appeared in published proceedings of conferences have been considered as journal articles, but when conference proceedings are unpublished or not generally available, the papers have been classified as technical reports.

The physical phenomena that govern propagation -- refraction, diffraction, and reflection (multipath) -- are treated in separate sections. The final section describes some simple propagation models that combine the fundamental physical phenomena, and Appendices A and B describe computer programs for these models.

Notwithstanding the work that has been done on VHF, UHF, and microwave propagation, there remain a number of fundamental, unanswered questions that are crucial to the complete understanding of low-altitude propagation. These questions concern the reflection properties of slightly rough surfaces at low

1

grazing angles, including the reflection coefficient of various kinds of vegetative ground cover (see Section 4) and problems associated with multiple diffraction effects along a terrain profile (see Section 5).

2. THE PATTERN PROPAGATION FACTOR

In this section we formulate the propagation problem associated with a surface radar searching for incoming aircraft at very low altitudes. We consider a radio frequency range from about 100 MHz to 10,000 MHz (VHF through X-band) and assume a geometry in which the radar site has been selected for optimum coverage and the radar antenna mounted at a height of 30 m or less above local terrain. The aircraft, we assume, will fly at some altitude between 30 and 150 m above ground level. This search geometry clearly represents an extreme case of low-angle propagation.

Propagation effects are taken into account in the radar equation by introducing the pattern propagation factor F. We designate the transmitted and received powers by P_t and P_r respectively, the effective aperture and gain of the radar antenna by A and G, the range by R, and the backscatter cross section of the target by σ, so the radar equation is

$$P_r = \frac{P_t \, AG}{(4\pi)^2} \ \frac{\sigma}{R^4} \ F^4 \qquad (2.1)$$

Here the pattern propagation factor is defined as

$$F = \frac{\text{Electric Field Propagated to the Target}}{\text{Electric Field at Same Range in Free Space}} \qquad (2.2)$$

Equation (2.1) is in the form given by KERR (1951), page 31. The principle of reciprocity makes it unnecessary to distinguish between the pattern propagation factor from radar to target and the factor from target back to radar. These two factors are equal and both are represented by F. In the case of one-way propagation over a range R, the received power is proportional to F^2 and R^{-2} rather than F^4 and R^{-4} in the two-way (radar) case. Reciprocity thus justifies applying the results of telecommunication studies to the problem of

2

radar detection, but we must keep in mind that, for example, a 20-dB excess loss, although acceptable for some communication purposes, becomes an excessive 40-dB loss in the radar case.

Referring to the radar equation, we can see that if propagation over terrain is compared to propagation in free space, the difference in return power from the target, measured in decibels, is given by 40 log F. Alternatively, if a minimum detectable return power $P_r(min)$ is specified, then the maximum detection range in free space, R_{max}(free space), is given by

$$R_{max}(\text{free space}) = \left(\frac{P_t \; AG}{(4\pi)^2} \; \frac{\sigma}{P_r(\text{min})} \right)^{1/4} \tag{2.3}$$

and for propagation over terrain, the maximum range becomes

$$R_{max} = F \; R_{max}(\text{free space}) \tag{2.4}$$

Hence, F is the factor by which the maximum detection range in free space is altered by propagation effects.

3. REFRACTION EFFECTS

The index of refraction n of the atmosphere depends on the pressure P, the temperature T, and the partial pressure of water vapor e. Over the frequency range with which we are concerned, the index of refraction is essentially independent of frequency and given by

$$n = 1 + N \; 10^{-6} \tag{3.1a}$$

where

$$N = 77.6 \; (P/T) + 3.73 \times 10^5 \; (e/T^2) \tag{3.1b}$$

Here P and e are expressed in millibars and T in degrees Kelvin. The quantity N, the radio refractivity, is commonly referred to as being expressed in N units as given by Eq. (3.1b). The quantities P and T can be measured directly, but the water-vapor content is usually measured indirectly by hygrometers (relative humidity), psychrometers (wet-bulb temperature), or dew-point devices

3

(dew-point temperature). With any of these measurements, the saturation
vapor pressure is required to convert the measured quantity to vapor pressure.
Figure 3.1 shows the saturated vapor pressure of water plotted as a function of
(T-273), the temperature on the Celsius scale. The contribution of the water-
vapor component to the radio refractivity must be relatively small for cold air
because the saturated vapor pressure is small as Fig. 3.1 shows. But for warm
air the relative humidity has a strong influence on the value of N.

Fig. 3.2 shows the radio refractivity at sea level as a function of tempera-
ture for relative-humidity values 0, 30, 70, and 100 percent. We see that
the water-vapor component of the refractivity increases exponentially with
increasing temperature.

There is no corresponding humidity component in the atmospheric index of
refraction at optical wavelengths*. For visible light the water-vapor com-
ponent makes a comparatively negligible contribution to the refractivity, so our
experience with the atmospheric bending of light rays generally does not apply
in the radio domain.

Now the deviations from rectilinear propagation will be determined by the
variations in radio refractivity in the atmosphere through which the wave
travels. The dominant variations will occur in the vertical direction with the
pressure, and usually the temperature and vapor pressure of water, decreasing
with increasing height above the ground. If the atmosphere is well mixed, that
is to say the air mass has been thoroughly mixed by convection, eddy turbulence,
and molecular diffusion and is in a state of mechanical equilibrium (gravita-
tional and buoyant forces balanced), then we can conveniently specify the
variations in P, T, and e with height. Let us describe the water-vapor content
in a well-mixed atmosphere by the specific humidity α, where

$$\alpha = \frac{M_w}{M + M_w} \tag{3.2}$$

*The electric dipole moments of water molecules can be reoriented by a radio
frequency electrical field, but at optical frequencies the field reverses
direction too rapidly for the water molecules to follow.

4
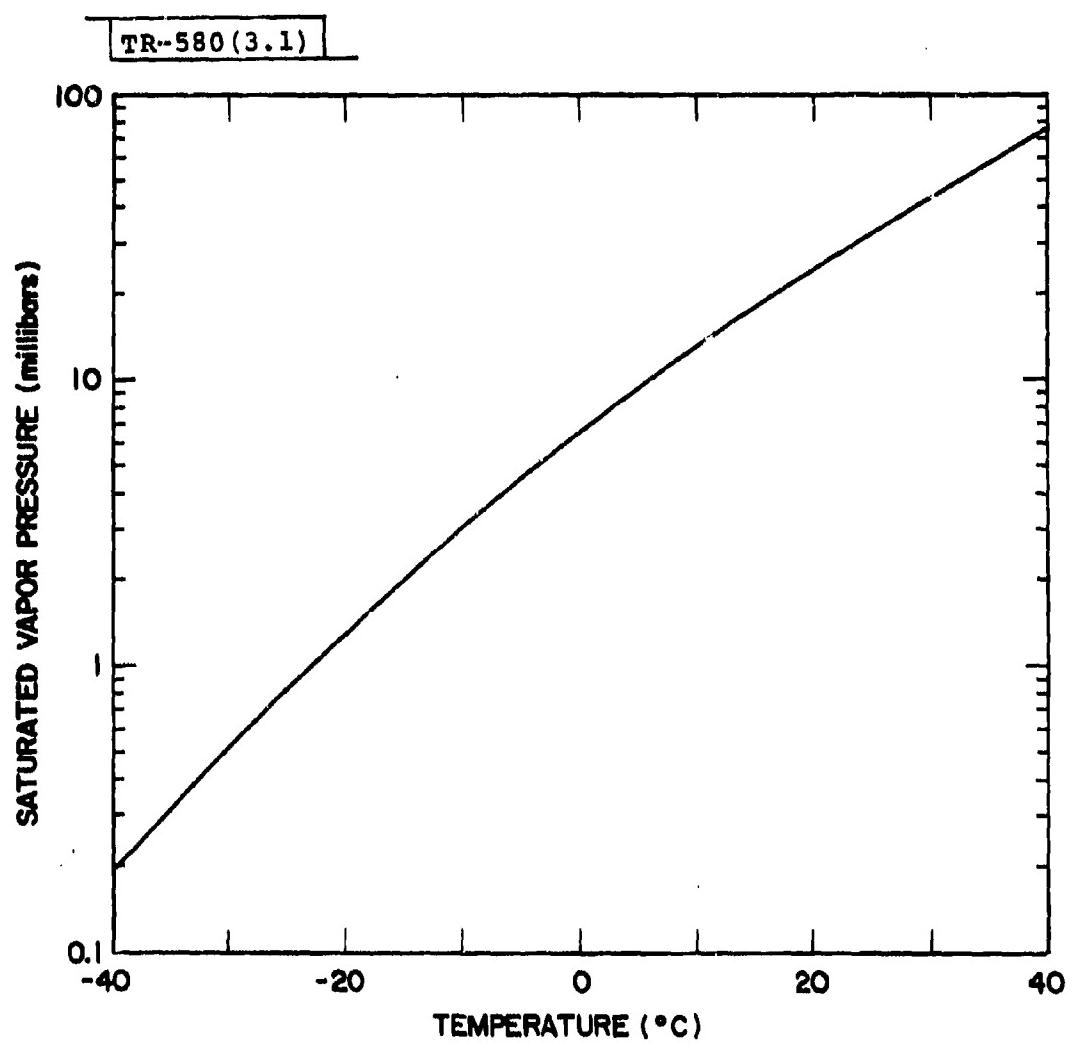
Fig. 3.1 The saturated vapor pressure of H_2O in millibars vs. temperature (Celsius). Over the temperature range from -40°C (-40°F) to +40°C (104°F) the pressure of saturated water vapor increases by nearly three orders of magnitude.
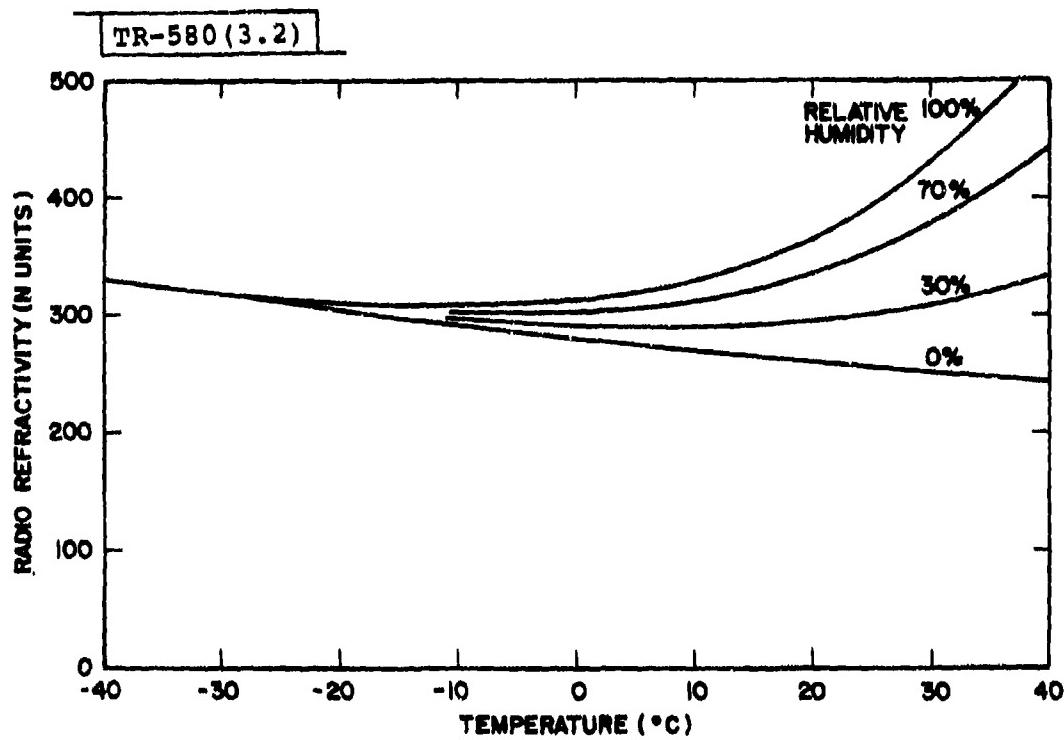
Fig. 3.2 The radio refractivity of air at a pressure of one atmosphere for four values of relative humidity. As the temperature rises the humidity can play an increasingly important role in determining the refractivity of the atmosphere.

and M_w and M are respectively the mass of water vapor and the mass of dry air in a given volume. Fig. 3.3 shows a family of curves that specify the refractivity as a function of elevation for several values of specific humidity within the range frequently encountered in practice.

Fig. 3.3 reveals three significant facts concerning the variation of N with elevation in a well-mixed atmosphere:

(1) The slope dN/dh, known as the refractivity gradient has nearly the same numerical value, -0.0082 N/ft or -27 N/km, throughout the range of values of H and α in the figure. This property provides the basis for a simple and convenient method for tracing the path of a wave front through a well-mixed atmosphere.

(2) The curves of refractivity vs. height are not quite straight lines, but dN/dh become slightly less negative as height increases. However, this curvature is not large enough to affect the validity of the standard ray-tracing method.

(3) The radio refractivity N is a strong function of α and increases rapidly as the specific humidity increases (see also Fig. 3.2). Hence, we can expect large changes in refractive effects in cases where the atmosphere ceases to be well mixed, and the temperature is high enough for the air to contain an appreciable amount of water vapor (see Fig. 3.1).

In all cases there is an upper limit to the height of well-mixed regions. The upper limit occurs when the temperature reaches the saturation value for the particular value of the specific humidity. This upper bound can be recognized visually as the height at which clouds appear.

Since the refractivity N decreases with height, as Fig. 3.3 shows, we expect qualitatively that the effect of refraction will be to bend horizontal rays downward and carry the radio waves to some extent around the curved earth. Rather than repeat the detailed analysis of the ray-tracing problem, which must be solved in this case, we shall state the results of this analysis. [The reader is referred to LIVINGSTON (1970), Chapter 4, for a clear exposition.]

7
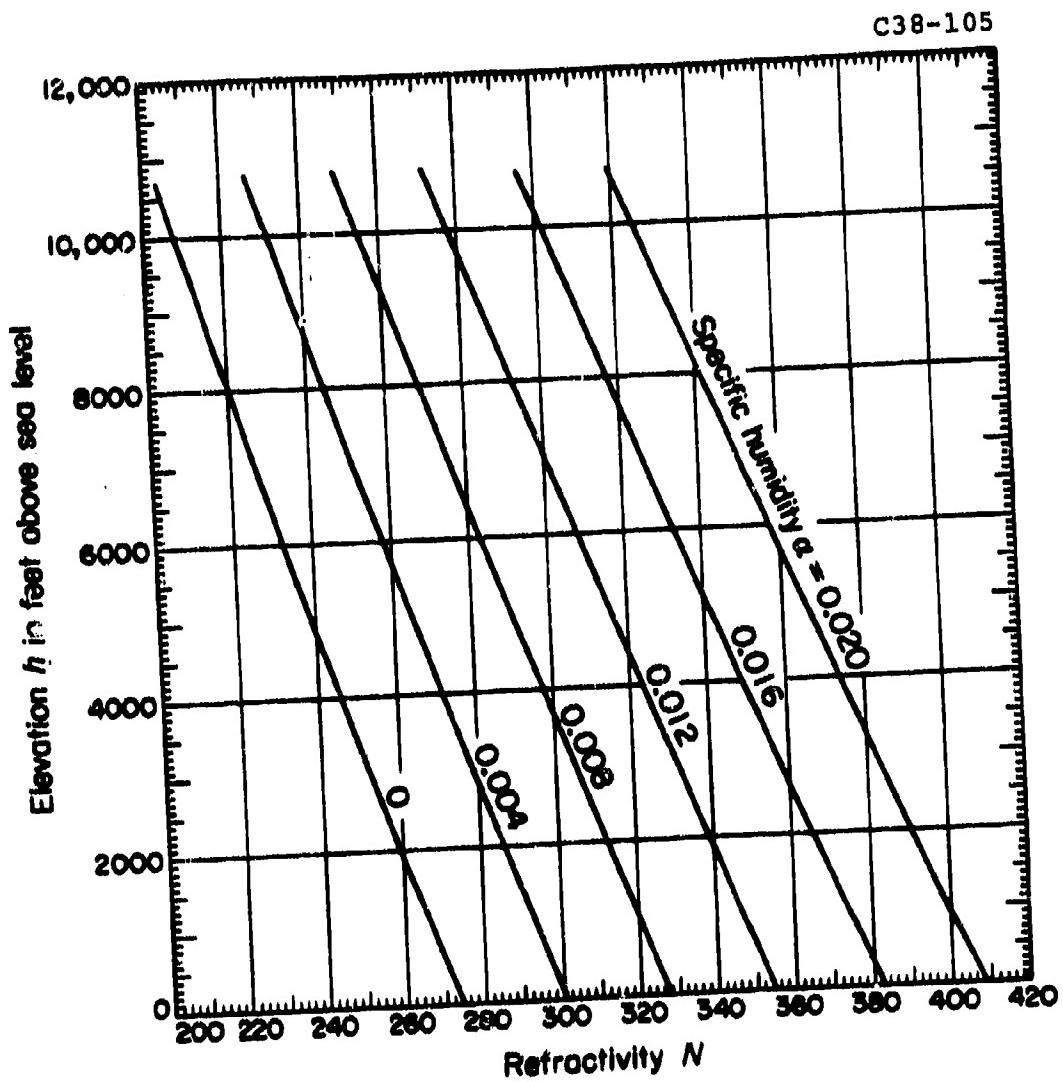
Fig. 3.3 Variation of refractivity with elevation in well mixed atmospheres for several values of specific humidity. The vertical gradient of the refractivity dN/dh is approximately -0.007 ft^{-1} throughout the range of h and α represented here. This figure is taken from LIVINGSTON (1970), page 65.

8

It turns out that the refractivity gradient dN/dh causes the nearly horizontal rays to be bent with a radius of curvature ρ given by

$$\rho = \frac{n}{-\frac{dn}{dh}\cos\psi} \tag{3.3}$$

where ψ is the angle that the ray makes with the horizontal. It was seen in Fig. 3.3 that dN/dh is nearly constant in a well-mixed atmosphere, and so from Eq. (3.1a) the quantity dN/dh must therefore be effectively constant. It follows then that the radius of curvature ρ must be constant for all rays close enough to the horizontal that cos ψ ≈ 1. Hence, the rays in which we are interested will be arcs of a circle of constant radius ρ. This circumstance allows us to make use of an ingenious geometrical transformation: the actual radius of the earth R_e (6370 km) is replaced by an effective radius KR_e such that we can represent the refracted rays as straight lines. The factor K which accomplishes this transformation is given by

$$K = \frac{\rho}{\rho - R_e} . \tag{3.4}$$

Now in terms of the vertical gradient of index of refraction n (or radio refractivity N), we can express K as

$$K = (1 + \frac{R_e}{n}\frac{dn}{dh})^{-1} = (1 + 10^{-6} R_e \frac{dN}{dh})^{-1} \tag{3.5}$$

Here we have made use of the fact that n is very nearly equal to one as can be seen from Fig. 3.2. For a well-mixed atmosphere, the refractivity gradient is about -27 N/km and K = 1.2. It has been customary, however, to adopt K = 4/3 as a standard working value, giving rise to the term 4/3 - earth atmosphere. But the well-mixed atmosphere would be a 6/5 - earth atmosphere. In practice, however, radiosonde measurements of atmospheric structure show that K can assume a variety of numerical values. The appropriate value of K will depend on geographical location, and with changing weather conditions at a given location, one can expect appreciable day-to-day changes in K as well.

9

Of course, atmospheric structure is by no means limited to cases in which the refractivity gradient is constant. Temperature inversions and humidity lapses may occur to produce highly variable refractivity profiles. For example, evaporation from the surface of the sea at low latitudes may lead to comparatively large values of the specific humidity in a shallow layer near the sea surface. Referring to Fig. 3.3 we can understand how this mechanism could produce large values of N near the surface with a drier otherwise well-mixed atmosphere above. If in this example the magnitude of the refractivity gradient becomes large enough, Eq. (3.3) shows that the radius of curvature ρ may become sufficiently small for a ray to be bent around the curve of the earth or even down to reflect forward from the surface of the sea. This process occurs to produce a so-called evaporation duct in which radio waves can propagate beyond the horizon. McCue (1978) has given a complete account of this phenomenon and its implications for low-altitude propagation at Kwajalein.

Many other atmospheric processes can lead to ducting and greatly extended propagation. Basically, ducting can occur when there is a transition from comparatively high refractivity near the surface to distinctly lower refractivity values above. In low and middle latitudes the air temperature, particularly in summer, may be high enough for the water-vapor component to play an important role (see Fig. 3.2). However, when the temperature is low, the atmosphere can contain only a small amount of humidity even when saturated. Hence in winter at higher latitudes, ducting must be a consequence of temperature inversions.

There are then at least two situations in which extended detection ranges over continental land masses may be expected due to refraction effects. Following rain the evaporation of water on the ground can produce an over-land evaporation duct. This phenomenon is, in fact, observed by weather radars (private communication, R.K. Crane). Ground clutter is found to spread out to much greater ranges when the ground is wet and when there is little wind. A totally different effect may be expected at high latitudes on clear nights over snow-covered terrain. Radiational cooling at the surface can produce a strong

10

temperature inversion and, therefore, anomalous propagation (Nottarp, 1967).
This high-latitude phenomena however will be restricted to clear nights when
there is no wind to mix the air near the ground. But in both of these cases,
the ducting will be less effective in increasing detection ranges over land
than over water because the reflectivity of the ground or snow surface will be
less than that of a calm sea or lake surface.

The widely accepted procedure for characterizing the effects of atmos-
pheric refraction on radio propagation in the design of ground-to-ground com-
munication systems is to use balloon-borne radiosonde measurements to estimate
the change ΔN in refractivity between the ground and an altitude of 100 m above
the ground. This value ΔN for the first 100 meters of height is then used to
estimate dN/dh in Eq. (3.5) and, thereby, to calculate K. The deficiencies in
this procedure are mainly the result of the fact that a radiosonde is not
designed to make accurate low-altitude measurements. However, one can obtain
some insight into the variability of refraction effects at various geographical
locations because the radiosonde soundings are usually made at 12-hour inter-
vals for meteorological purposes. The distribution of the values of $\Delta N/\Delta h$
and K for sites in Canada and the northern States have been published by Segal
and Barrington (R 1977), and selected worldwide measurements of refractivity
gradients have been published by Samson (R 1976) for use in designing line-of-
sight communication systems.

Fig. 3.4 shows two examples of the probability distributions of ground-
based refractivity gradients and K values based on radiosonde measurements for
Edmonton, Alberta, and Inuvik, Northwest Territories, taken from the report of
Segal and Barrington (R 1977). These plots show separately the distributions
for three-month intervals starting in January. Note that the values of K,
reading downward in these plots, become increasingly large and change over to
negative numbers. This happens because as $\Delta N/\Delta h$ becomes increasingly negative
in Eq. (3.5) the expression in parentheses goes to zero, making K = ∞ when
$\Delta N/\Delta h$ = -157 N/km. For this value of the refractivity gradient the ray curva-
ture becomes equal to that of the earth. Even more negative values of $\Delta N/\Delta h$

11
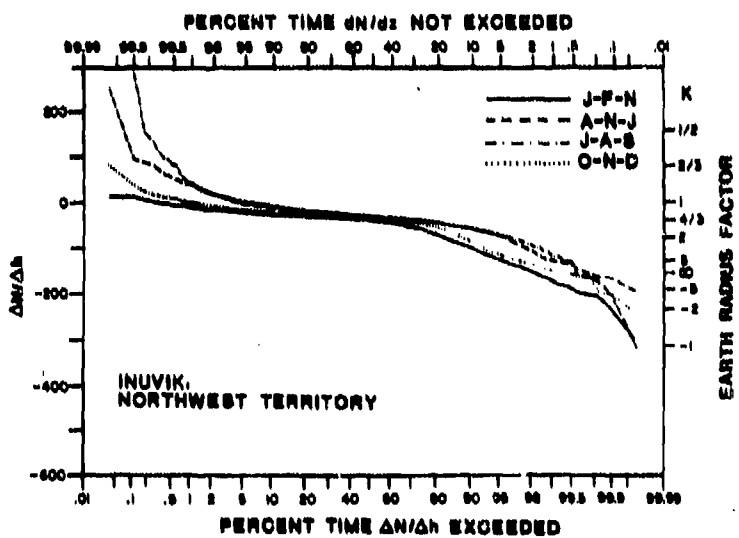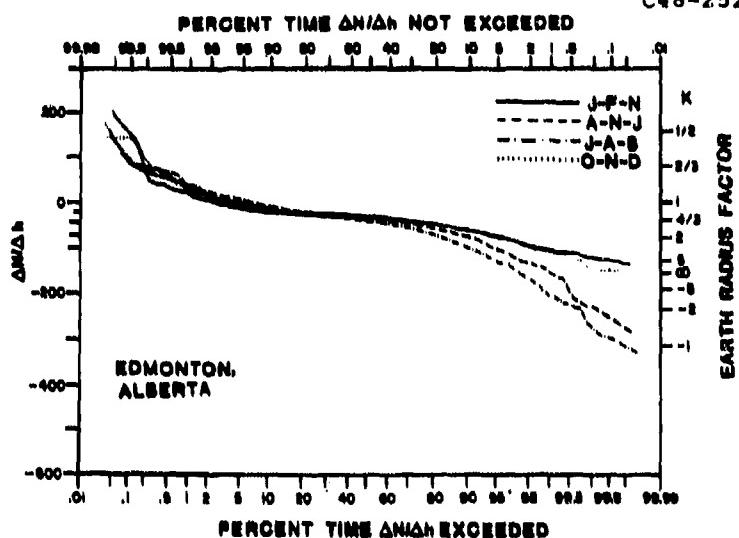
Fig. 3.4 Two examples showing the seasonal frequency of occurrence of refractivity gradients and K values. The refractivity gradients for these Canadian sites in N-units/km were determined for the lowest 100-m layer of the atmosphere from radiosonde measurements. These curves were taken from Segal and Barrington (R1977).

12

produce negative values of K, situations in which ducting would be expected to occur.

From the examples in Fig. 3.4 we can obtain estimates of the frequency of occurrence of various values of K. At both Edmonton and Inuvik the values of K lie between one and two during 80 percent or more of the year. At Edmonton, K exceeds two or becomes negative (ducting condition) most frequently during July-September when these conditions occur about 20 percent of the time. At Inuvik the same conditions for extended propagation range (K > 2 or K < 0) occur during January-March when the frequency of occurrence is about 20 percent. Abnormally shortened ranges (0 < K < 1) are relatively uncommon in these examples, being present 5 percent of the time or less at both sites.

Up to this point we have not considered the absorption effects of rain and atmospheric gases on the propagation of radio waves. Measurable rainfall occurs less than 5 percent of the time except in coastal areas (see Samson, R 1976), and rain attenuation has not been included within the scope of this report.

A convenient summary of the phenomena of rain attenuation has been given by R.K. Crane in Section 2.4 of MEEKS (1976). Figure 3.5 shows plots of the attenuation one-way in dB/km as a function of frequency for rain (three different rain rates), for typical clouds, and for fog; this figure appears as Figure 1 (p. 178) in the reference cited to MEEKS (1976). For radio frequencies VHF through X-band the droplets are small compared to wavelength λ, and the scattered power is proportional to λ^{-4} (Rayleigh scattering) when the droplet circumference becomes comparable with or larger than λ the scattering becomes proportional to the geometrical cross section of the droplet and is nearly independent of λ as we see in Fig. 3.5.

Absorption by atmospheric gases is negligible at frequencies below about 10 GHz compared to the uncertainties of low-angle propagation even in the most predictable situations. However, significant amounts of absorption may occur at frequencies above 10 GHz. Absorption by atmospheric gases in the frequency

13
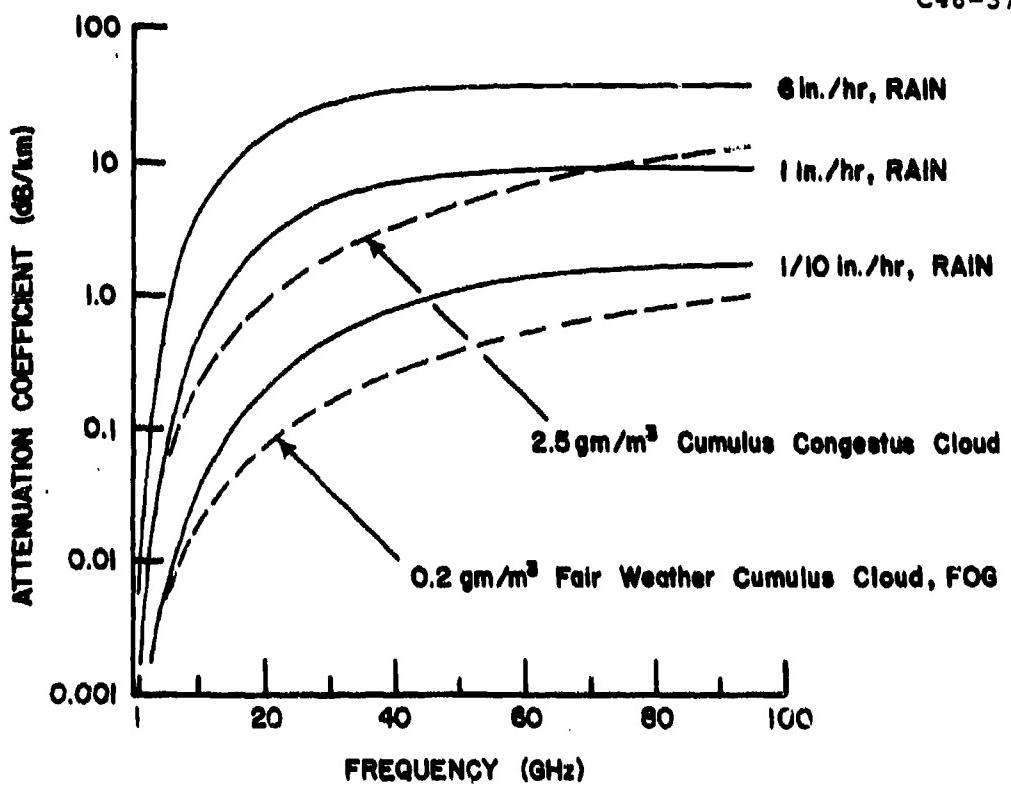
Fig. 3.5   Attenuation coefficient vs. frequency for rain, clouds, and fog.

range from 10 to 300 GHz is thoroughly discussed by J.W. Waters in Section 2.3 of MEEKS (1976).

4. REFLECTION AND ABSORPTION EFFECTS OF TERRAIN

4.1 Introduction

In studying the propagation of radio waves at low-elevation angles over the surface of the earth we must take into account forward scattering (or multipath effects). We consider first reflections from idealized dielectric surfaces in the form of smooth planes (Section 4.2). Such surfaces produce only coherent reflections. Then we consider the more complicated problem of reflections from rough surfaces where both coherent and diffuse scattering can occur (Section 4.3). Finally, we discuss briefly absorption effects of trees and other vegetation which may cover terrain.

4.2 Reflection Coefficient for a Smooth Plane Surface

When a wave encounters a smooth plane surface which is very large in extent compared to a wavelength, specular reflection takes place and the angles of incidence and reflection are equal (Snell's law). For our propagation geometry the waves move in a nearly horizontal direction, and we shall use the common terminology as follows: vertical polarization refers to linear polarization with the electric field vector lying in the vertical plane containing the incident and reflected rays, and horizontal polarization refers to linear polarization with the electric field horizontal.

The reflection coefficient Γ is defined as the ratio of the amplitude of the reflected wave to the amplitude of the incident wave. The classical formulas derived first by Fresnel in 1816 give the reflection coefficients for horizontal and vertical polarization as a function of the dielectric constant and conductivity of the ground substance. It is convenient to define a relative complex dielectric constant ϵ_r as follows:

$$\epsilon_r = \frac{\epsilon}{\epsilon_o} - 60 \ i \ \lambda \sigma \qquad (4.1)$$

where ε is the dielectric constant, σ the conductivity in mhos per meter of the ground, ε_0 the dielectric constant of free space, and λ the wavelength in meters. The reflection coefficient will furthermore be a complex quantity

$$\Gamma = \rho e^{-i\phi} \tag{4.2}$$

where ρ and ϕ give the amplitude and the phase shift of the reflected wave with respect to the incident wave.

Rather than repeat the Fresnel equations here, we shall present only the computed reflection coefficients as a function of angle in graphical form for representative types of ground and for sea water. Table 4.1 gives the appropriate constants for several types of soil and water. We have evaluated the Fresnel equations for very moist ground, average ground, polar ice, and sea water. The equations themselves may be found in BECKMANN AND SPIZZICHINO (1963), pages 218-219, or in KERR (1951), pages 396-403. The direction of the incident wave is specified here by the grazing angle ψ, the angle between the incident ray and its projection on the horizontal reflecting plane. Horizontal and vertical polarization reflect differently, so we show here the results of computations for horizontal and for vertical polarization, respectively; the magnitudes of the reflection coefficients ρ_h and ρ_v and their phase lags ϕ_h and ϕ_v. Figure 4.1 shows these quantities plotted for average ground, for very moist ground, and for polar ice, which has nearly the same parameters as very dry ground (see Table 4.1).

Qualitatively the reflection parameters show similar behavior as a function of grazing angle for various values of the surface-material parameters. We will summarize the characteristics of the reflected waves using Figure 4.1 as our example. (1) The magnitude of the reflection coefficient for horizontal polarization ρ_h has the value one at very small grazing angles and decreases monotonically as ψ increases. (2) The coefficient for vertical polarization ρ_v on the other hand has a single, well-defined minimum which is $\rho_v = 0$ provided $\sigma = 0$. The corresponding grazing angle for a perfect dielectric is given by $\sin^{-1}(1/\sqrt{\varepsilon/\varepsilon_0})$, and the complement of this angle is called Brewster's polarizing

TABLE 4.1

APPROXIMATE ELECTROMAGNETIC PROPERTIES OF SOIL AND WATER*

Type of Surface	ϵ/ϵ_o	$\sigma(mhos/m)$
Seawater at 0°C	80	4-5
at 10°C	73	4-5
Fresh water at 10°C	84	$1 \times 10^{-3} - 1 \times 10^{-2}$
at 20°C	80	$1 \times 10^{-3} - 1 \times 10^{-2}$
Very moist ground	30	$5 \times 10^{-3} - 1 \times 10^{-2}$
Average ground	15	$5 \times 10^{-4} - 5 \times 10^{-3}$
Arctic land	15	5×10^{-4}
Very dry ground and large towns (industrial areas)	3	$5 \times 10^{-5} - 1 \times 10^{-4}$
Polar ice	3.	2.5×10^{-5}

*From FINK (1975), pp. 18-79. Additional data on electromagnetic properties are contained in references cited in the Subject Index under 8. Reflection effects electrical properties of surface materials.
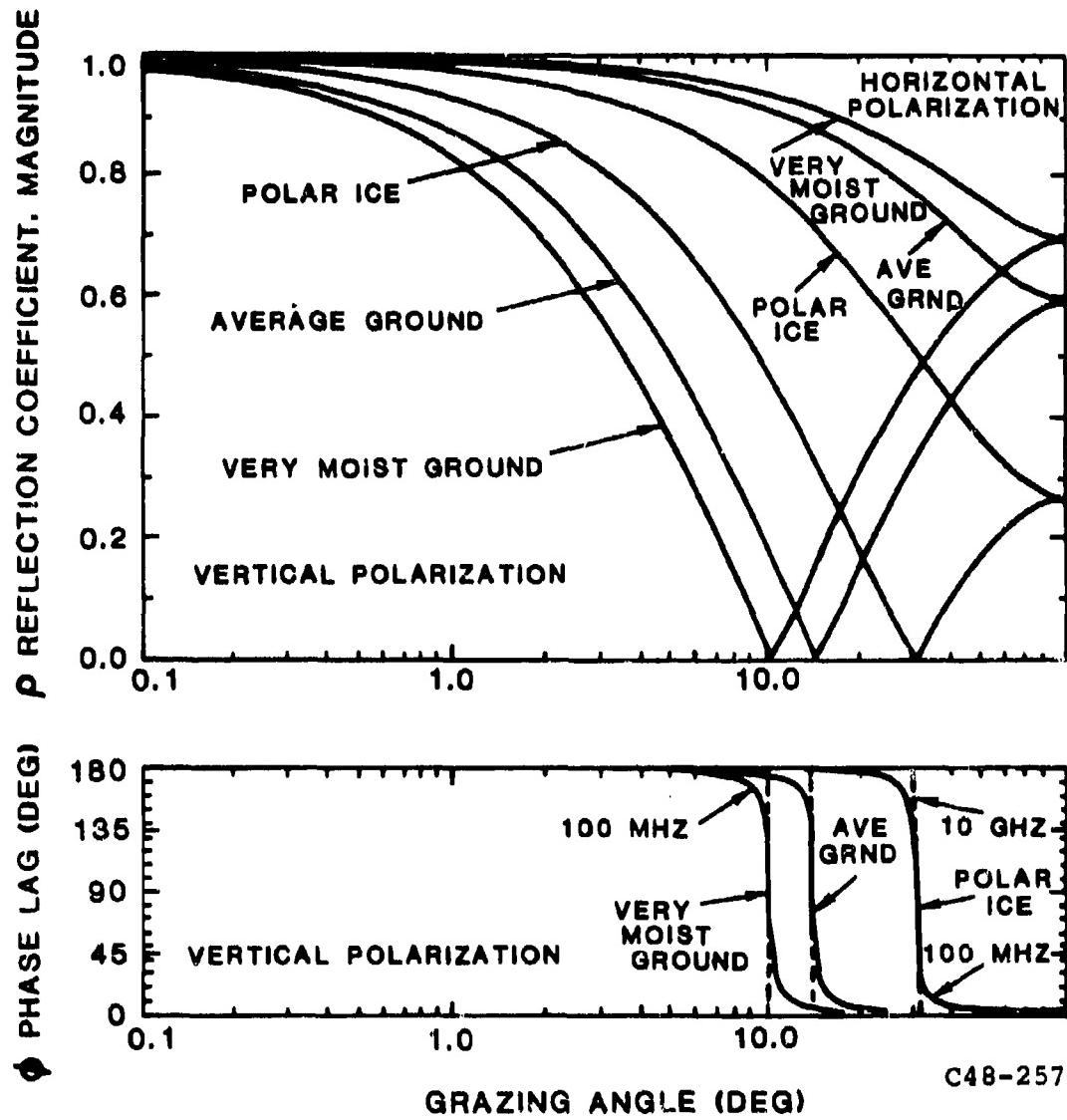
Fig. 4.1 The reflection coefficient as a function of grazing angle for very moist ground, average ground, and polar ice. The relative dielectric constant and conductivity for each surface material are given in Table 4.1. Values of ρ and ϕ in Eq. (4.2) were computed for frequencies of 100 MHz and 10 GHz. These frequencies gave identical curves for ρ, but somewhat different curves for ϕ.

angle*. (3) For horizontal polarization the phase lag ϕ is nearly π for all values of ψ, but for vertical polarization of the phase lag ϕ goes from π at small grazing angles ($\psi \leq 8^\circ$) to zero for large grazing angles ($\psi \geq 45^\circ$) with the changeover occurring abruptly around Brewster's angle. (4) For very low grazing angles, ψ in the neighborhood of one degree or less, both ρ_h and ρ_v are nearly one and ϕ_h and ϕ_v are nearly π. As a result, there should be little difference in the propagation of horizontally and vertically polarized waves over ground at very low grazing angles. The conclusion is borne out by many propagation experiments (for example, LaGrone (1960), McPetrie and Ford (1964), and Oxehufwud (1959)), but two exceptions should be noted: over a cylindrical ridge of large radius of curvature, vertical polarization diffracts somewhat deeper into the shadow zone (see Section 5.3), and the trunks of trees in a forest scatter vertical polarization more than horizontal when the wavelength is large compared to the diameters of tree trunks. (5) The electromagnetic properties of the various ground types all lead to effectively the same reflection coefficient at very low grazing angles as Fig. 4.1 shows.

On the other hand, sea water which has a comparatively high conductivity shows somewhat different reflection characteristics. Fig. 4.2 gives the reflection coefficient of sea water at three frequencies as a function of grazing angle. As one goes to lower frequencies, the imaginary part of the complex dielectric constant of sea water increases as Equation 4.1 specifies, and for vertical polarization the minimum in ρ_v shifts to lower angles and becomes less pronounced. Also the phase lag ϕ_v makes a more gradual change from zero to π as ψ increases.

The special case of smooth reflecting surfaces discussed in this section can be used to represent actual terrain reflectivities in at least three cases: (1) ocean or lake surfaces with negligible wave disturbance, (2) flat desert surfaces, and (3) snow-covered plains. It turns out for vertical polarization that snow and sand have quite similar reflection properties at grazing angles below Brewster's angles as shown in Fig. 4.3. Nevertheless, in the great

---

*This effect can be used to advantage in the design of airborne radars which look down for low-flying targets. By employing vertical polarization such radars can eliminate or greatly reduce multipath due to ground reflections.
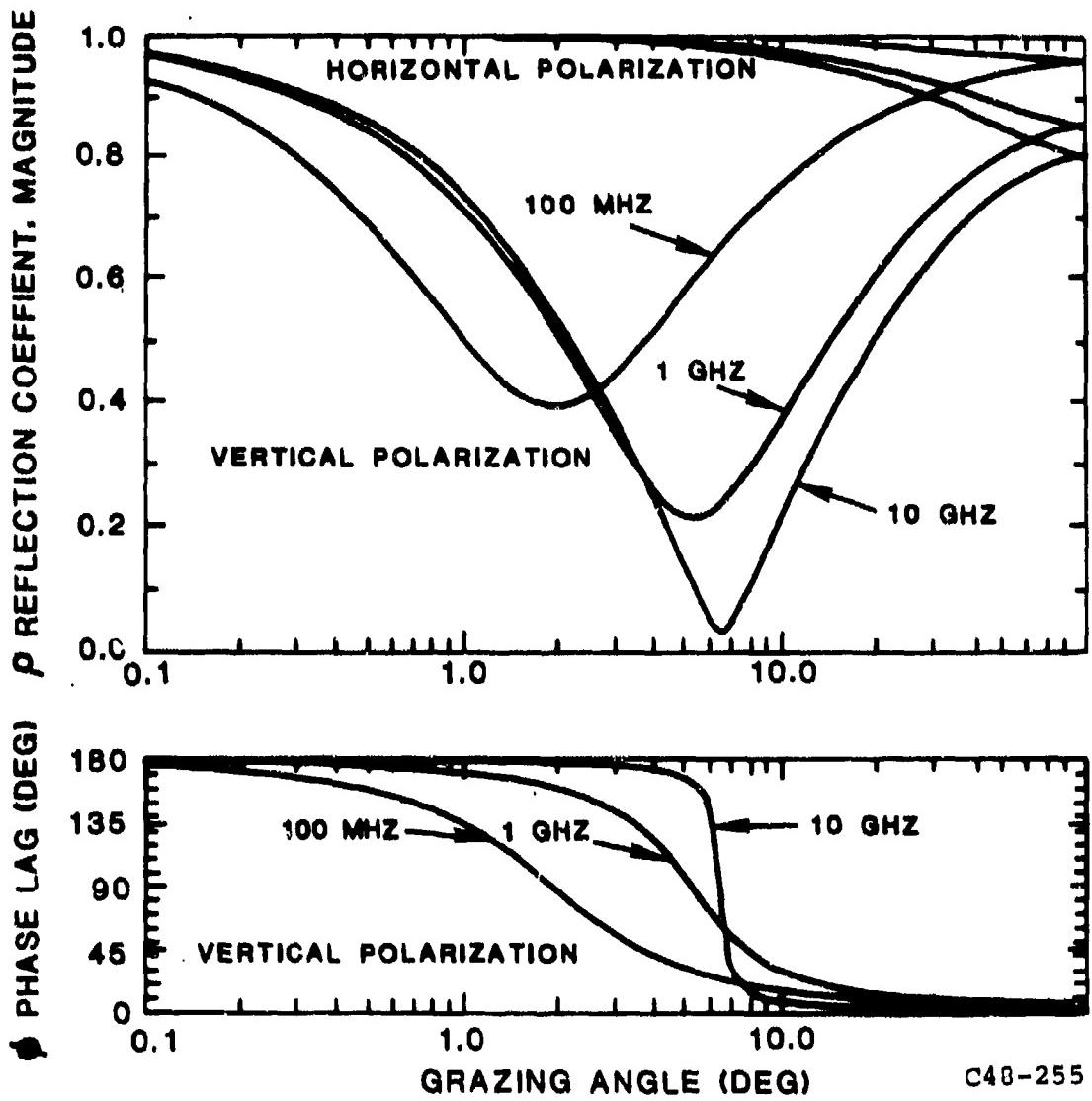
Fig. 4.2 The reflection coefficient as a function of grazing angle for sea water. The relative dielectric constant is 80 and the conductivity 5.0 mhos/m Separate curves are shown for frequencies of 100 MHz, 1 GHz, and 10 GHz.

20
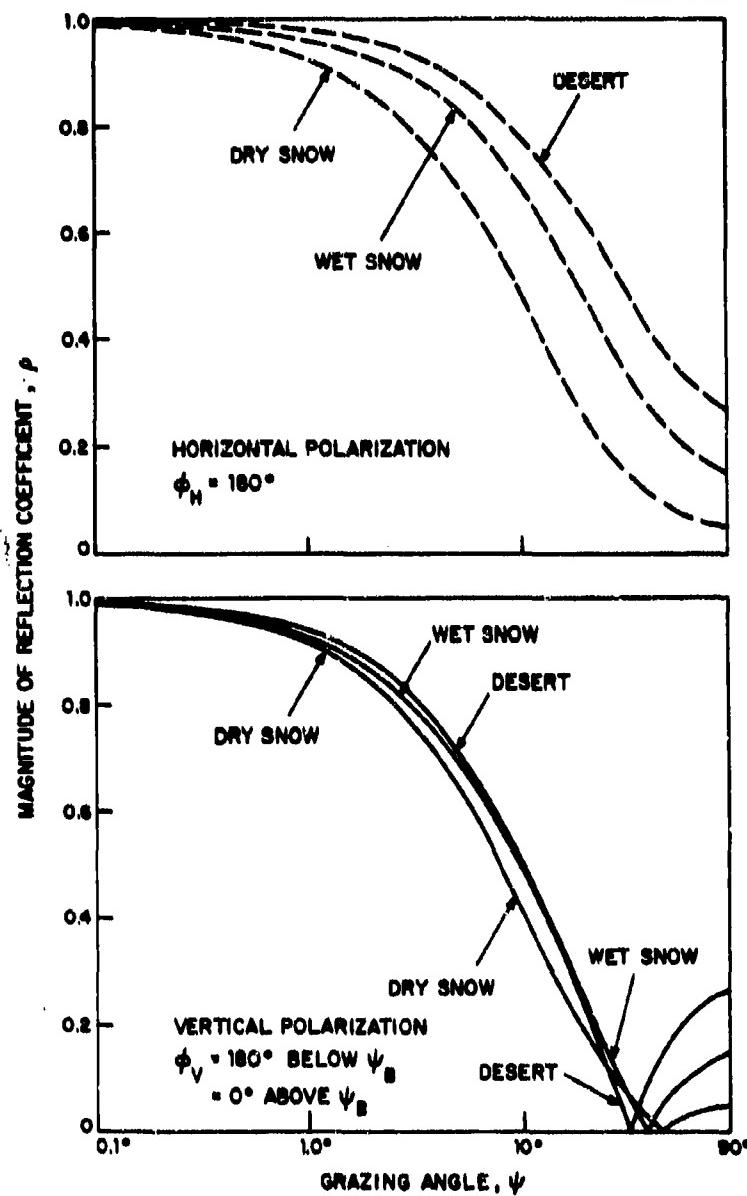
Fig. 4.3 The reflection coefficient as a function of grazing angle for dry snow, wet snow, and sand. The assumed values for the relative dielectric constant were 1.2, 1.8, and 3, respectively. A conductivity of 0.1 mhos/m was assumed in all three cases. Brewsters angle is designated by ψ_B.

majority of cass actually encountered the ground is not smooth, and we must find ways to take into account not only the gross terrain surface features, but also the small-scale local roughness and vegetative cover.

4.3 Reflections from Rough Surfaces

When an electromagnetic wave propagates at low angles, the direct wave combines with waves reflected from the ground so that the target is illuminated by a complex wave front. We now consider the nature of ground reflections that must be taken into account if we are to predict propagation under realistic conditions, that is over a rough terrain surface. Let us think of the terrain as a large collection of scatterers distributed so as to represent the reflection properties of the surface features. If we examine the phase of the individual waves arriving at the target from these scatterers, we will find, in general, that a fraction of the phases will be found to be randomly distributed (diffuse scattering) and the remainder will be strongly correlated in phase (coherent scattering). In the discussions that follow we shall neglect the diffuse scattering. We do so because the signals from the diffuse scatterers combine with random phases and add up to produce a field strength that is negligible in comparison to the direct wave. On the other hand, coherent scattering, depending on the nature of the terrain, can produce a reflected wave comparable in amplitude with the direct wave. (In fact, if the terrain should happen by chance to have a surface of nearly spheroidal contour, the reflected waves could be brought to a focus at the target, producing a reflected wave much stronger than the direct wave.) Coherent reflection may or may not be produced depending on the roughness of the terrain and the wavelength of the signal, but if coherent reflection occurs, the reflected wave will propagate in the same azimuthal direction as the direct wave. On the other hand, diffuse reflections will scatter energy in all directions. In the backward direction the diffuse reflection of course produces the backscattered ground clutter seen by the radars.

The characteristics of specular and diffuse reflection are well described in the following paragraphs from BECKMANN and SPIZZICHINO (1963), page 241.

22

"Specular reflection is a reflection of the same
type as caused by a smooth surface: it is directional
and obeys the laws of classical optics. Its phase
is coherent and it is the result of the radiation of
the points on the Fresnel elipse, which transmit
waves of approximately equal phases toward the
receiver. Its fluctuations have a relatively small
amplitude.

Diffuse scattering is a phenomenon that has little
directivity and which consequently takes place over
a much larger area of the surface than the first
Fresnel zone. Its phase is coherent and its fluctuations,
which have a large amplitude, are Rayleigh-distributed."

The existence of these two components of the reflected field is well established
by optical as well as radio experiments.

A simple theoretical model has been developed to calculate the specular
reflection coefficient R_s of rough terrain. Because of the assumed randomness
of the terrain, R_s must itself be random with an RMS value given by

$$(R_s)_{RMS} = (\rho_s)_{RMS} \; \Gamma \tag{4.3}$$

Here ρ_s is the scattering coefficient and Γ is the reflection coefficient for a
smooth-plane earth. For a Gaussian-model rough surface, according to BECKMANN
and SPIZZICHINO (1963), page 246, we have

$$< |\rho_s|^2 >_{average} = e^{-(\Delta\phi)^2} \tag{4.4}$$

with

$$\Delta\phi = \frac{4\pi \; \Delta h \; \sin\psi}{\lambda} \tag{4.5}$$

The model surface is specified by the single parameter, Δh which is the standard
deviation of the normal distribution of heights measured from a plane surface.

ψ is the grazing angle, and λ is the wavelength. The quantity $\Delta\Phi$ is just the phase difference between two rays that reflect from the rough surface: one ray reflecting from the mean surface level and the other from a bump of height Δh on the surface.

This simple theoretical model is in reasonable agreement with actual measurements (see BECKMANN and SPIZZICHINO, 1963, pp 317, 303) over a range of grazing angles that goes below one degree. However, the propagation measurements with which the model can be compared permit only relatively crude estimates of Δh, and it does not appear useful to consider more elaborate models until more complete and accurate propagation data with quantitative ground truth are obtained.

Notwithstanding the limitations of the Gaussian terrain model, it is useful to examine those combinations of radio wavelength and terrain type for which this model predicts appreciable coherent reflection. Let us consider an idealized case of propagation over a spherical earth with homogeneous surface roughness specified by Δh. Figure 4.4 shows a diagram in which Δh and λ appear as the x- and y-axes. Also indicated in this figure are the terrain-type and seastate designations that roughly correspond to various ranges of values of Δh. These terrain roughness designations are the ones used by Longley and Rice (R 1968). We have fixed values of ρ_s and ψ and plotted on the diagram the locus of $(\Delta h, \lambda)$ values that would give rise to specific values of scattering coefficient at specific grazing angles. These loci from Eqs. (4.4) and (4.5) must appear on the diagram as diagonal straight lines, all with the same slope. We represent two cases in Fig. 4.4. For both cases we assume nominal values for the height of the radar antenna (30 m) and for the altitude of the target above ground (90 m). At a comparatively short range of 10 km over a spherical earth, the grazing angle of the reflected ray is 0.7°, and at a longer range of 30 km the grazing angle (spherical earth) is 0.2°. On the diagram in Fig. 4.4 we have plotted two bands with the left edge of each band corresponding to $\rho_s = 0.9$ (largely specular reflection) and the right edge to $\rho_s = 0.3$ (largely diffuse reflection). The reflection coefficient R_s in Eq. (4.3) is, of course, determined by ρ_s since at these low grazing angles $\Gamma = 1$ (see Section 4.2). These

24
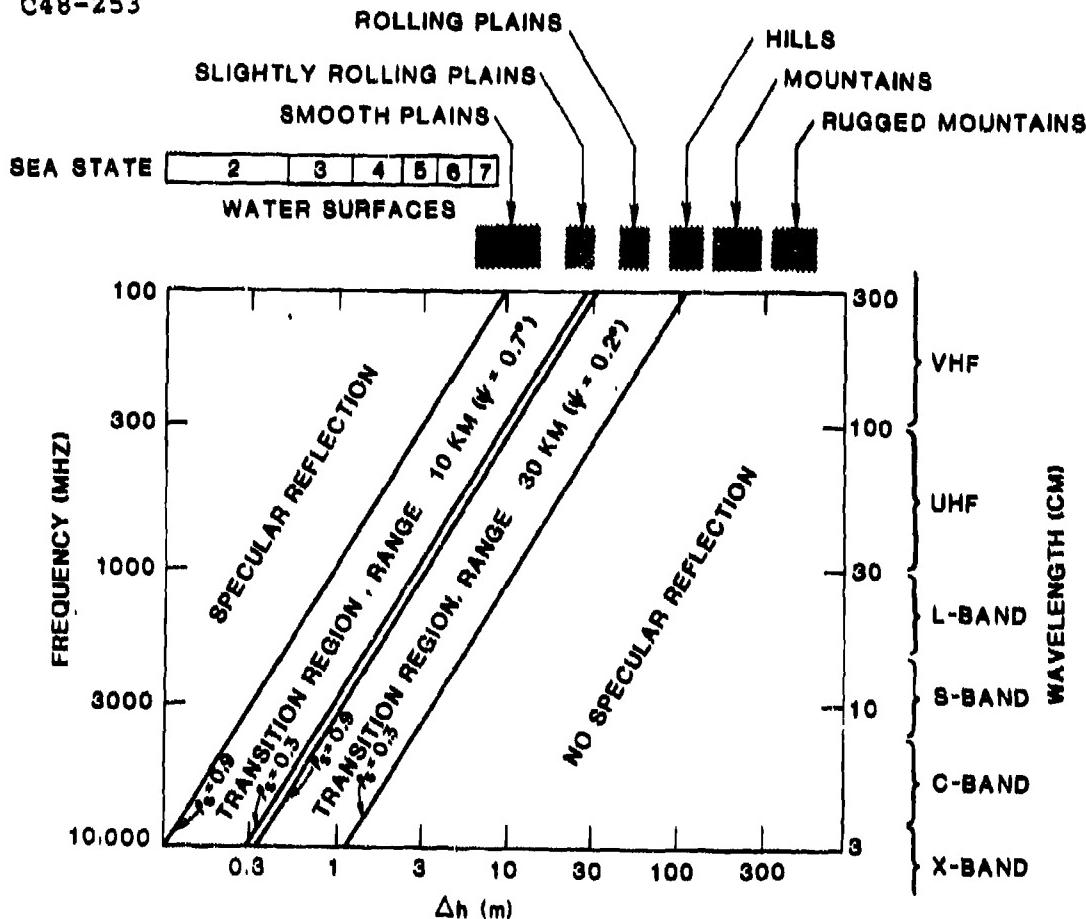
Fig. 4.4 Terrain-wavelength diagram showing the combinations of Δh and radio frequency for which appreciable specular reflection is predicted by the Gaussian terrain model. Two diagonal bands are shown representing the transition regions between specular and diffuse terrain reflection for assumed target ranges of 10 and 30 km. In both cases the antenna and target heights are 30 and 90 m.

bands represent transition regions between the upper-left region in Fig. 4.4, where the terrain reflection is specular and the lower-right region where the reflection is entirely diffuse. For the shorter range of 10 km, this model predicts that high reflectivity would be expected only for low VHF frequencies over smooth plains and for VHF and UHF frequencies over water. For the longer range of 30 km, the highly reflective regions are extended to include slightly rolling plains for VHF frequencies and smooth plains for UHF frequencies. The increased reflectivity for the longer range is a consequence of the factor $(\sin \psi)$ in Eq. (4.5). For all landforms with which we are concerned, excluding very unusual cases, the value of Δh will always be greater than 3 m. So, on the basis of this model, we can rule out appreciable specular reflection from terrain when the microwave bands are used (i.e., frequencies greater than 1 GHz). Table 4.2 summarizes the types of terrain that may produce appreciable coherent reflection in the various wavelength bands.

In summary we can say that coherent-reflection effects will be most important at VHF and UHF frequencies, where the reflection coefficients may approach one. On the other hand, at X-band, C-band, and S-band we can expect, in almost all cases, low values of reflection coefficient, $R_s \leq 0.3$.

It should be emphasized that the Gaussian terrain model considers ρ_s as a random variable and predicts the RMS value of ρ_s so we should expect measured values of the reflection coefficient to show fluctuations as the target position changes by small amounts. Since the model treats reflection properties of rough surfaces as statistical quantities, the most we can expect is that the model will predict statistical measures of R_s. This model, of course, has serious limitations, but nevertheless in the future even better models must of necessity be statistical in character. In principle if we had a very complete quantitative description of the terrain, we should be able to predict R_s accurately, but in practice the terrain must be characterized by statistical quantities unless we are willing to work with very small terrain samples.

Up to this point we have not considered specifically the effects of vegetative cover on the reflection properties of terrain. In general these effects

TABLE 4.2

PREDICTED OCCURRENCE OF SPECULAR REFLECTION ($R_s \geq 0.5$)

Radar Band	Type of Reflection Predicted
X-band (8 - 12.5 GHz)	Appreciable specular reflection only for Sea States ≤ 2 (R = 30 km). Overland scattering is entirely diffuse.
C-band (4 - 8 GHz)	Appreciable specular reflection for Sea States ≤ 2 (R = 10 km) and ≤ 3 (R = 30 km). Overland scattering is entirely diffuse.
S-band (2 - 4 GHz)	Appreciable specular reflection for Sea States <4 (R = 30 km). Overland scattering is effectively diffuse.
L-band (1 - 2 GHz)	Appreciable specular reflection for Sea States ≤ 5 and for land with $\Delta h < 5$ m (R = 30 km); otherwise diffuse reflection.
UHF (300 - 1000 MHz)	Appreciable specular reflection from Smooth Plains* and all Sea States for R = 30 km.
VHF (30 - 300 MHz)	Appreciable specular reflections from Smooth Plains* and Slightly Rolling Plains* for R = 30 km.

*The terrain types cited here are indicated in terms of Δh in Fig. 4.4; these are the terrain categories of Longley and Rice (1968).

27

are not well understood, but there are two groups of measurements that shed some light on the problem. At a frequency of 4 GHz we have the results of measurements made by the American Telephone and Telegraph Co. during the engineering of the transcontinental microwave-relay system (Bullington, 1954). These measurements were made over a series of paths (each roughly 25 miles long) that form links in a communication chain connecting New York and Denver. In most cases, the reflection coefficients fell in the range from 0.2-0.4. The paragraph below from Bullington's paper describes the comparison of ground-reflection data for vegetated and barren paths.

> "The data on the New York-Omaha section of the route was
> separated from the Omaha-Denver section to show whether or
> not the difference in the type of terrain adds significantly
> to the spread in the overall results. At first, some of the
> low-reflection coefficients were attributed to absorption
> in the numerous trees along some of the paths, but an ap-
> proximately equal percentage of low reflections were found
> in the relatively flat, treeless areas in eastern Colorado."

At longer wavelengths, a different situation emerges. Extensive measurements have been made of television service fields at VHF and UHF frequencies. The standard receiving antenna height for these measurements is 30 ft, a height small compared to radar antenna heights or target heights. Nevertheless, these experimental results must be considered relevant. The following paragraphs are quoted from a survey paper, LaGrone (1960).

> "Vegetation is an important factor in field-measured data at
> some television frequencies.... At low VHF (frequencies), it was
> found to be negligible (in its effect), but at high VHF (fre-
> quencies), trees and tall grasses were found to absorb a
> significant amount of the signal."

and

"The absorption of radio waves by trees and grasses noted at
higher VHF (frequencies) was found to be considerably more
at UHF. Previously it was noted that trees thick enough
to block vision were essentially opaque at 1000 MHz."

The comparatively small effect of vegetation on VHF propagation is qualitatively
confirmed by the fact that at 67 MHz no appreciable change in television cover-
age is found between summer and winter conditions in the Boston area (private
communication, Joseph Blake, Chief Engineer, WBZ-TV, Channel 4). Clearly more
experimental work will be required to understand the effects of vegetative cover,
particularly at UHF frequencies, for antenna (or target) heights from 100 ft to
500 ft, rather than 30 ft.

5. DIFFRACTION EFFECTS

5.1 Introduction

It is the nature of waves to bend around obstacles. This diffraction
phenomenon plays a central role in the propagation of radio waves at low ele-
vation angles over the ground. Hills and ridges diffract energy into the
shadow zone and make possible radio communication and radar target detection
within these zones. Theoretical models that describe diffraction by a knife-
edge and by cylinders with various radii of curvature may be used in predicting
radio propagation, and the areas of application and limitations of these simple
geometrical models are fairly well understood. In this chapter we discuss
these models.

In the theoretical analysis of diffraction, the obstacles are frequently
chosen to be perfect conductors and the polarization of the electromagnetic
waves may be an important consideration. However, for knife-edge diffraction
the results are rigorously independent of polarization, and for cylinder dif-
fraction the polarization dependence, although strong for perfect conductors,
is small for the values of dielectric constant and conductivity encountered on
terrain at our frequencies of interest. In this chapter we shall assume that
the polarization is horizontal (i.e., the electric vector is perpendicular to

29

the plane containing the incident and diffracted rays). For diffraction by cylinders, Hacking (1970) has confirmed experimentally that vertical polarization propagates somewhat more strongly into the shadow zone than horizontal polarization, but the difference is small (≤ 2 dB).

We shall consider in the sections that follow the Fresnel-Kirchhoff calculation of diffraction by a knife-edge and the corrections that must be added when it becomes necessary to account for the finite radius of curvature of the diffracting mask. It turns out that most hills and ridges can be well represented by a knife-edge. In the final section we discuss the problem of successive diffraction over several knife-edges.

The diffraction models which we discuss in this chapter are essentially two-dimensional models, so a question arises concerning the widths that obstructions must have perpendicular to the plane of incidence for these models to apply. The answer to this question is that the obstruction must have a transverse width greater than the first-Fresnel-zone width,

$$\sqrt{\lambda\ d/4}\ \ [1 - (\frac{2d_1}{d}) - 1)^2]^{1/2}$$

where d is the distance from the radar to the target (or transmitter to receiver), and d_1 is the shorter of the two distances: radar to obstruction and obstruction to target. For an obstruction centered on a 10-km path, the first-Fresnel-zone widths are 87 m, 27 m, and 9 m for radio frequencies 100 MHz, 1 GHz, and 10 GHz, respectively.

5.2 Diffraction by a Knife-Edge

The problem of diffraction of an electromagnetic wave by a knife-edge is a classical problem in optics solved by Sommerfield in 1896, and the detailed solution is given in BORN & WOLF (1959), Sections 8.7 and 11.5. The geometry of the problem is illustrated in Fig. 5.1.

Here we consider first one-way propagation from a transmitter at T to a receiver at R over a knife-edge at O. An important parameter is the clearance of the line TR over the knife-edge or, if the line TR intersects the mask,
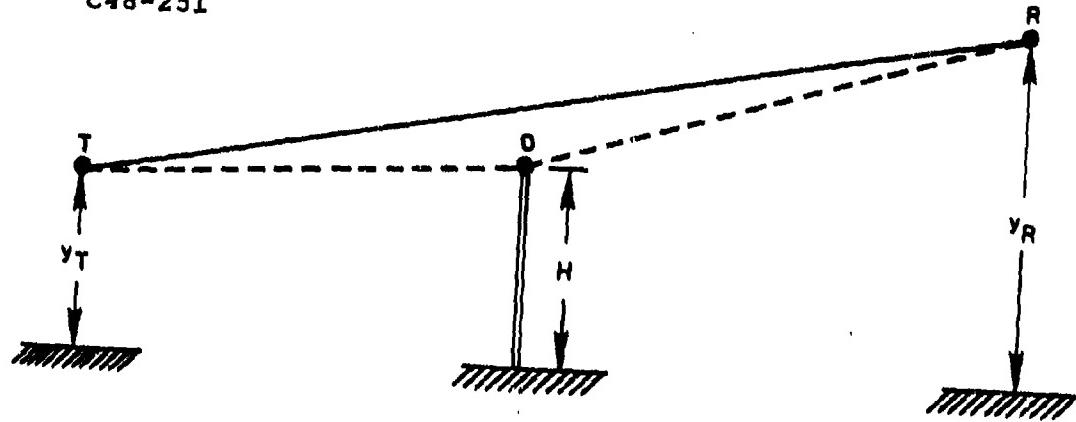
Fig. 5.1 The geometry of the diffraction problem.

(a)

(b)
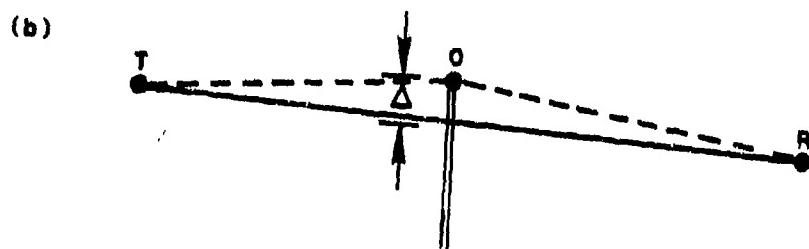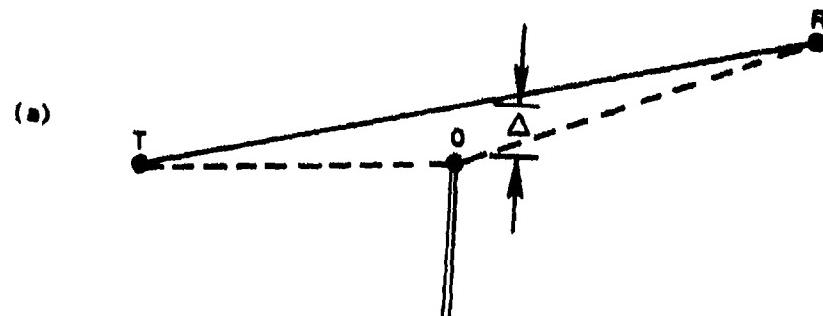
Fig. 5.2 The clearance parameter Δ. (a) shows an example of positive clearance, and (b) shows negative clearance.

31

the distance from 0 to TR. We call this clearance distance Δ, taking Δ as positive when TR clears the mask and as negative when TR intersects the mask (R in the shadow region). Figure 5.2 shows this definition of Δ.

The solution to the knife-edge diffraction problem gives the field at R due to a source at T, and from the principle of reciprocity the same field would be produced at T if the transmitter were placed at R. Accordingly, we consider the transmitter and knife-edge as fixed and denote the field at the receiver as $E(d_R, y_R)$. The explicit solution $E(d_R, y_R)$ for wavelength λ near the geometric shadow (for either polarization) is given by

$$E(d_R, y_R) = \frac{e^{-i(\pi/4)}}{\sqrt{2}} e^{ikr} \{[\tfrac{1}{2} + C(w)] + i [\tfrac{1}{2} + S(w)]\} \qquad (5.1)$$

where:

$$k = 2\pi/\lambda$$

$$r = \sqrt{(y_T - y_R)^2 + (d_T + d_R)^2}$$

$$w = \sqrt{2} \left(\frac{\Delta}{\sqrt{\lambda\, d_T\, d_R/(d_T + d_R)}}\right) \qquad (5.2)$$

$$C(w) = \int_0^W \cos \tfrac{\pi}{2} \tau^2 \, d\tau$$

$$S(w) = \int_0^W \sin \tfrac{\pi}{2} \tau^2 \, d\tau$$

The functions $C(w)$ and $S(w)$ are the Fresnel integrals and their argument w has a simple geometrical interpretation. When the clearance Δ has the value Δ_o such that

$$\Delta_o = \sqrt{\lambda\, d_T\, d_R/(d_T + d_R)} \qquad (5.3)$$

then the path length TOR is longer than the direct path TR by an amount $\lambda/2$. Thus, Δ_o as defined above is just the clearance that puts the knife-edge at the boundary of the first Fresnel zone, and from Eq. (5.2) the Fresnel parameter w may be expressed as

$$\frac{w}{\sqrt{2}} = \frac{\text{clearance of ray TR}}{\text{clearance of first Fresnel zone}} = \frac{\Delta}{\Delta_o} \qquad (5.4)$$

In other words, $w/\sqrt{2}$ is just the clearance of ray TR expressed in units of the first-Fresnel-zone clearance. (A more detailed discussion of this problem is given in BRODHAGE & HORMUTH (1977), Section 3.1.)

Now let us look at the solution to the knife-edge diffraction problem given by Eq. (5.1). Figure 5.3 shows the power propagated from T to R relative to free-space propagation. This quantity expressed in decibels is equal to 20 log F, where F is the pattern propagation factor defined in Chapter 2.

The independent variable in this figure is just the ray clearance in units of Δ_o. Expressed in this way the result is, of course, independent of wavelength.

In order to see how radio waves of different frequencies diffract over a knife-edge, let us consider an example. Figure 5.4 shows the geometrical arrangement and a plot of the pattern propagation factor F computed as a function of the target height for five different radar frequencies (wavelengths): 100 MHz (3 m), 300 MHz (1 m), 1 GHz (30 cm), 3 GHz (10 cm), and 10 GHz (3 cm). It is convenient to interpret the quantity F as the factor that multiplies the maximum range of the radar in free space to obtain the maximum range under propagation conditions characterized by F (see Section 2, Eqs. (2.3) and (2.4)). Hence, a radar with a maximum range in free space of 150 km would be able to detect the target in Fig. 5.4 at a range of 15 km provided $F \geq 0.1$ in the absence of ground clutter. The curves plotted in Fig. 5.4 show that the target would be detectable at any height above the ground at radar frequencies below 300 MHz. However, for higher radar frequencies -- 1, 3, and 10 GHz -- the minimum heights for detection are 62, 91, and 100 m above the ground, respectively. This is, of course, a simplified example which neglects ground reflection and ground clutter. In Section 6 we consider the combined propagation effects of diffraction and reflection.

In the design of microwave links, careful consideration must be given to the diffraction effects of terrain. Field experiments (for example, Oxehufwud,
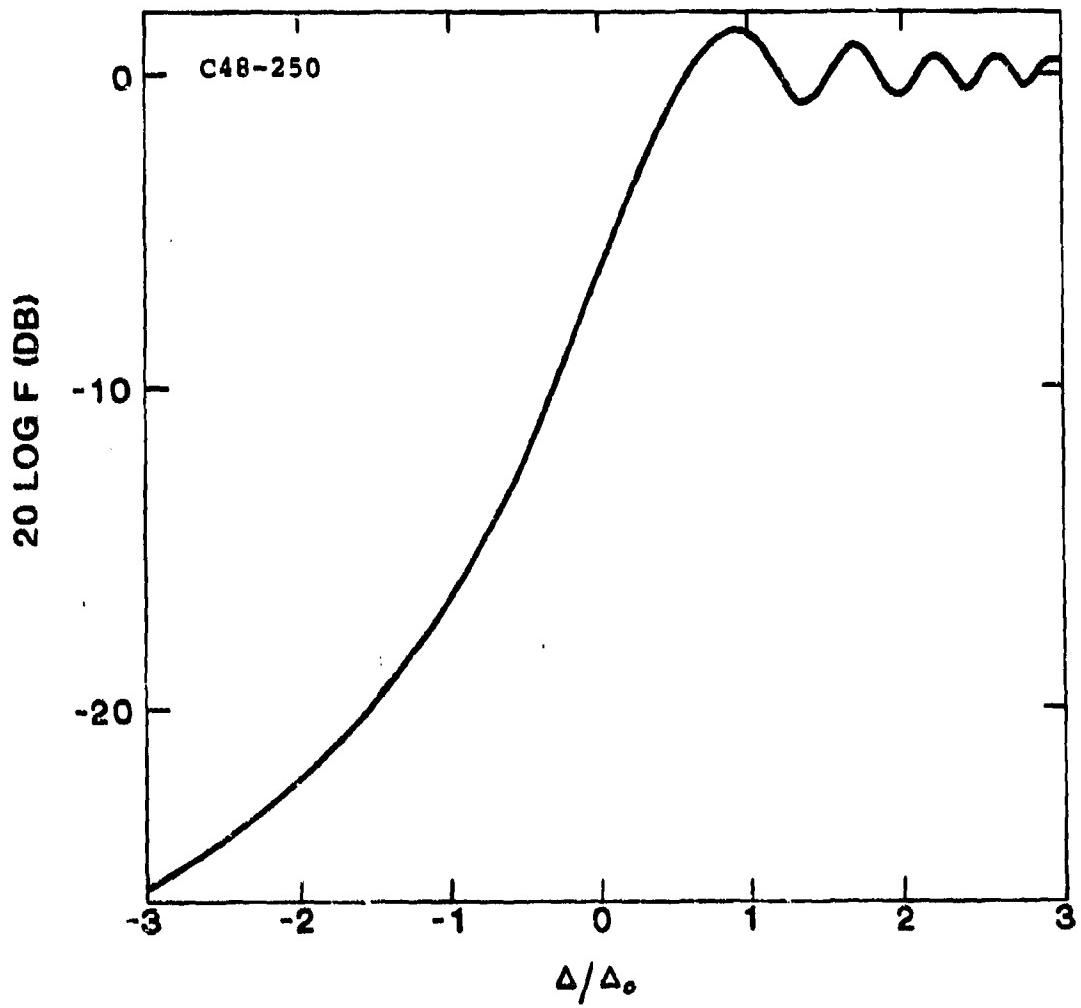
Fig. 5.3 Propagation over a knife-edge as a function of normalized clearance. The abscissa represents the clearance Δ normalized in units of first-Fresnel-zone clearance. The ordinate, 20 log F (F - pattern propagation factor, see Chapter 2), is also the one-way propagated power relative to free space expressed in dB.

C48-249

20 LOG F (DB)

100 MHZ
300 MHZ
1 GHZ
3 GHZ
10 GHZ

FREE SPACE
MAX RANGE 150 KM

0   50   100   150   200   250
TARGET HEIGHT (M)

F
1.0
0.8
0.6
0.4
0.3
0.2
0.1
0.08
0.06
0.04

0
-10
-20
-30

TARGET
HEIGHT

-135 M

100 M

30 M

0

10 KM   5 KM

NON-REFLECTING
GROUND
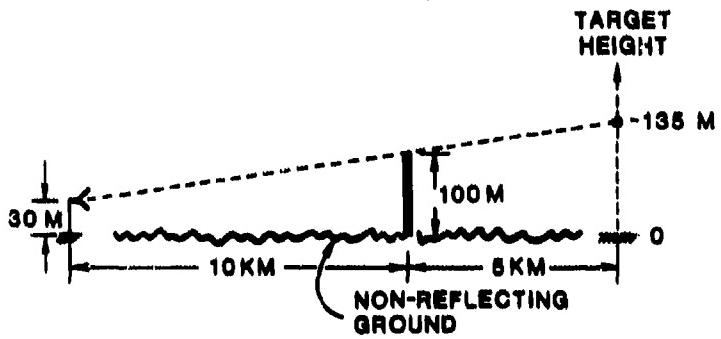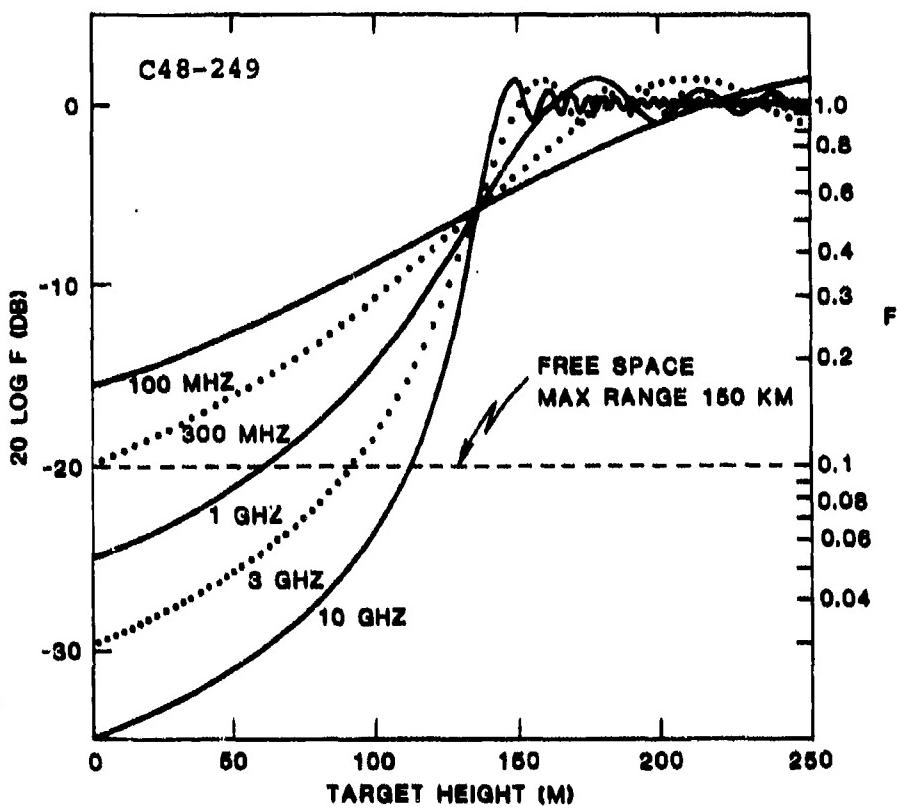
Fig. 5.4 An example of knife-edge diffraction for five radar frequencies. The absicssa of the graph represents target height as shown in the diagram. The ordinate represents both 20 log F and F, where F is the pattern propagation factor. The dashed horizontal line shows the detection limit for targets in the shadow region. Above this line a target could be detected (in the absence of clutter) by a radar with a maximum free-space range of 150 km.

1959) have shown that terrain obstruction will not be evident if 60 percent or more of the first Fresnel zone is unobstructed. Fig. 5.3 shows that for $\Delta/\Delta_o \geq 0.6$ the effect of knife-edge diffraction on one-way propagation would be no more than 1.5 dB. According to BRODHAGE & HORMUTH (1976), Section 4, the design practice is to place the antennas high enough that the first Fresnel zone is entirely unobstructed in order to allow for unfavorable atmospheric refraction conditions. Depending on the refractivity gradient in the atmosphere, the earth-radius factor K (see Section 3) will determine the effective clearance. In constructing computational models of low-angle propagation, one therefore has the support of theory and practice in neglecting diffraction for cases in which $\Delta/\Delta_o \geq 0.6$. In such cases we have what is referred to as Fresnel clearance.

5.3 Diffraction by Cylinders

In some situations a more appropriate model for diffraction by a hill or ridge is provided by the case of diffraction by a cylinder. Solutions to the problem of diffraction of electromagnetic waves around a cylinder have been given by Rice (1954), Neugebauer and Bachynski (1958), and by Wait and Conda (1959). We shall make use of the results of Dougherty and Mahoney (1964), who extended the solution of Wait and Conda (1959) and presented the results in convenient graphical form. Cylinder diffraction is presented in the form of corrections to be applied to the solution for a knife-edge. Dougherty and Mahoney (1964) use the dimensionless parameter ρ to characterize the effect of the finite radius of curvature of the cylinder. They define ρ as

$$\rho = \sqrt[6]{\frac{\lambda \, r^2}{\pi}} \sqrt{\frac{d_T + d_R}{d_T \, d_R}} \tag{5.5}$$

where r is the radius of curvature of the cylinder and λ is the wavelength. Fig. 5.5 shows the diffraction loss as a function of the normalized clearance Δ/Δ_o for six different values of ρ. The curve for $\rho = 0$ corresponds to the previous case of knife-edge diffraction. For a frequency of 300 MHz, for example, and a hill with radius of curvature 0.5 km forming an obstruction midway along

36
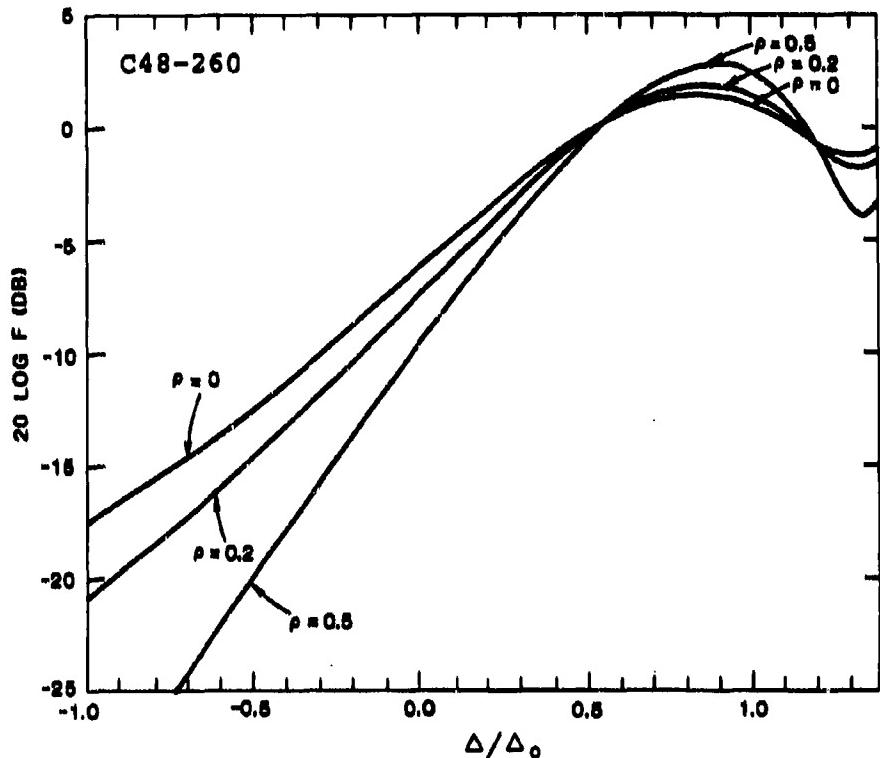
Fig. 5.5 Propagation over a cylinder as a function of normalized clearance. The parameter ρ, defined in Eq. (5.5), increases with increasing radius of curvature of the cylinder. Knife-edge diffraction corresponds to ρ = 0.

a 10-km path, we calculate from Eq. (5.5) the value $\rho = 0.131$. Referring to Fig. 5.4, we can see that for $\Delta/\Delta_o = -0.5$ the one-way diffraction loss is 12 dB for a knife-edge and 14 dB for the rounded hill. So, in this case, the rounded hill gives 2 dB more loss, a comparatively small change. For shorter ranges, Eq. (5.5) would give a larger value of ρ and greater excess loss for an obstruction of this shape. If we go to higher frequencies (shorter wavelength) we would find little decrease in ρ because λ enters only to the power 1/6; also the dependence on r goes as the power 1/3, which means that ρ is also not a strong function of r.

However, when the radius of curvature begins to approach an earth radius with the corresponding $\rho > 1$, the excess loss over that of a knife-edge may become very large. This circumstance leads to the concept of obstacle gain whereby propagation may actually be improved by erecting a knife-edge barrier near the center of a spherical-earth path. For example, Dickson, et al. (1953), reported that for one-way propagation on a 160-mile path over the 8,000-ft level of Mt. Fairweather in Alaska at a frequency of 38 MHz, the measured loss was 73 dB less than that calculated from smooth-earth diffraction theory, an "obstacle gain" of 73 dB. At VHF frequencies, according to Dickson, et al. (1953), it is commonly observed that very long paths over mountainous terrain provide good communication with negligible fading.

5.4 Multiple Diffraction

Radio waves propagating near the surface of the earth may frequently encounter more than one diffracting mask. The problem of multiple diffraction has been investigated by Millington, Hewitt, and Immirzi (1962) in the case of double knife-edges; their analysis, based on Fresnel diffraction theory, cannot easily be generalized to more than two successive knife-edges. However, Deygout (1966) has developed a semi-empirical procedure for predicting multiple diffraction losses which agrees with the results of Millington et al. for the double knife-edge and gives good agreement with propagation measurements over paths with up to five diffracting hills.

The Deygout method of calculation as reported in Deygout (1966) gives significantly better agreement with experiment than the methods of Bullington (1947) and Epstein and Peterson (1953).

We shall describe the Deygout method by showing an example in which three successive diffractions are handled. The method of computation can be understood as a straightforward generalization of this example. Fig. 5.6(a) shows the clearances of the three masks from the line TR. These clearances are by definition negative numbers. The principal mask must be determined by dividing the clearance h for each mask by its first-Fresnel-zone clearance for path TR and selecting the most negative Fresnel clearance as the principal mask. In this example M_2 is the principal mask. Next, we draw the paths to the the top of the principal mask, TM_2 and M_2R, and record $\Delta_2 = h_2$ as the clearance for the principal mask. Fig. 5.6(b) shows this step in the construction. Finally, we draw paths TM_1 and M_1M_2 and paths M_2M_3 and M_3R as shown in Fig. 5.6(c), and the appropriate clearances Δ_1, Δ_2, and Δ_3 are labeled. Note that Δ_3 is now a positive clearance. Now the excess path attenuation, one-way, can be computed by taking into account the clearances: Δ_1 for path TM_2, Δ_2 for path TR, and Δ_3 for path M_2R. The corresponding losses in decibels can be determined from Fig. 5.3 and added together to obtain the total excess loss.

Errors in the Deygout method of calculation may be estimated by comparing the attenuations calculated for two successive knife-edges by the Deygout method and the more rigorous method of Millington, et al. (1962). This comparison shows that the Deygout method overestimates the attenuation when the two knife-edges have nearly the same Fresnel-zone clearance considered separately. More specifically, errors will occur when the secondary mask has a Fresnel-zone clearance that is 70 percent or more of the Fresnel-zone clearance of the principal mask. If the two nearly equal masks are close together, the over-estimate produced by the Deygout method may approach 6 dB. Therefore, one must be careful when employing the Deygout method in cases where two or more prominent features in the terrain are close together and have nearly the same heights.

C43-256
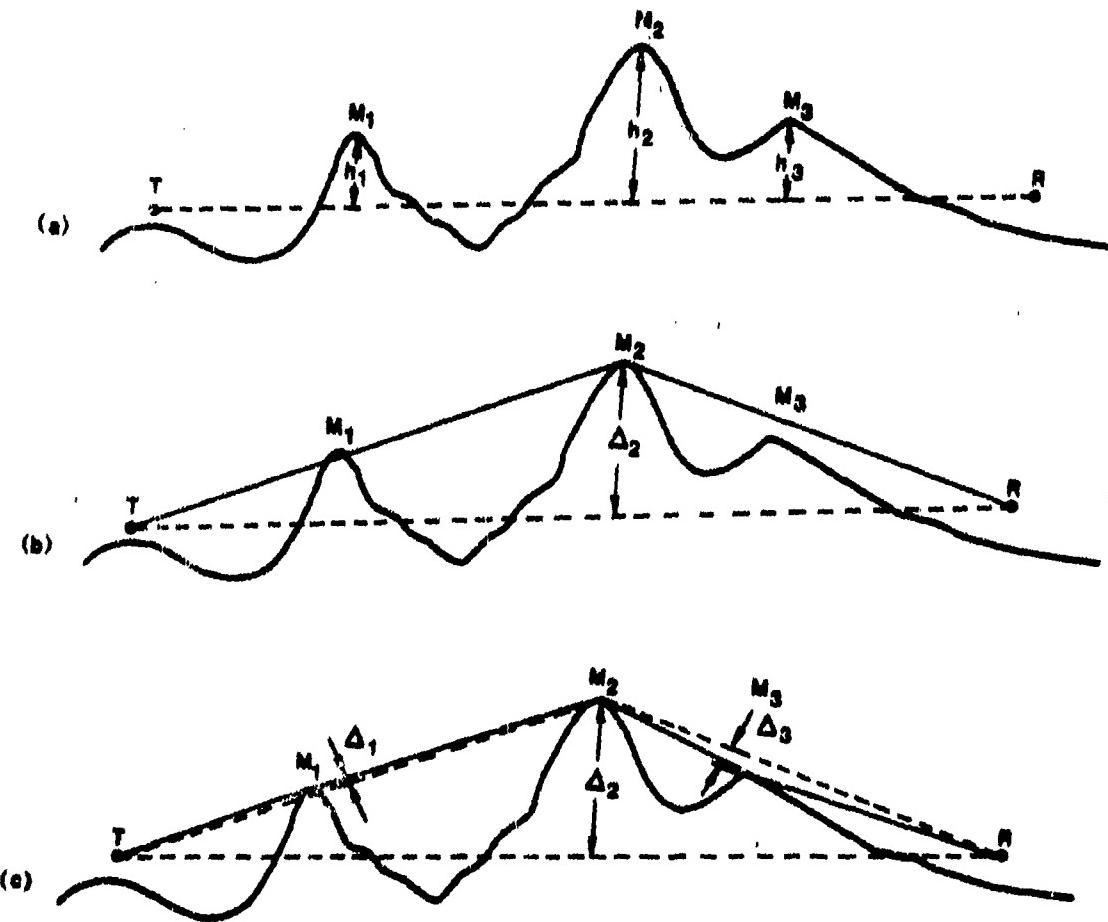
Fig. 5.6 An example of the Deygout construction. (a) shows the clearances from which the principal mask is determined, (b) shows the paths with respect to the smaller masks, and (c) shows the clearances used to calculate the attenuations of the three masks.

40

6. PROPAGATION MODELS

6.1 Introduction

Here we consider the problem of computing the signal strength propagated over a specific terrain profile taking into account the effects of refraction, reflection, and diffraction. Following the discussion of refraction in Section 3, we see that in most cases the downward bending of ray paths by the atmosphere can be taken into account by substituting for the actual curvature of the earth a modified radius of curvature that is somewhat larger. The factor 4/3 is commonly considered as the standard correction factor, but over land this factor varies with weather conditions lying between one and two roughly 90 percent of the time (see Section 3). Since maps describe the terrain relief with reference to sea level, one can correct the sea level elevations for earth curvature and refraction by adding a term as follows:

$$h_i = h_i(\text{map}) - \frac{x_i^2}{2 K R_e}$$

where: h_i = the height of an element of the terrain profile,

h_i (map) = the map height above sea level,

x_i = the distance from the radar to the element,

$K R_e$ = the modified earth radius.

In this way the terrain profile may be obtained with the refraction correction built in.

The influence of terrain reflection is not so easily taken into account. The discussion in Section 4 points out that appreciable coherent reflection from the ground can be expected only for terrain classified as plains, and primarily for radars operating in VHF or UHF frequency bands. However, the magnitude of the reflection coefficient will depend on the vegetative ground cover, and we lack an experimental basis for assigning reflection coefficients to common types of ground cover. Nevertheless, we can examine the effects of ground reflection in some particular cases by trying several values for the

41

reflection coefficient. In all terrain types except plains, diffraction by hills and ridges will be the most important phenomenon governing radio propagation at low altitudes. When there is a single diffracting ridge or hill along the path, the problem is easily handled with the methods described in Section 5. If there are several diffracting masks in series along the profile, the propagation may be calculated by the Deygout method which gives a good approximation in most cases (see Section 5.4). On the other hand, over smooth plains, radio waves reflect from and diffract over what is essentially a sphere (or cylinder) with a very large radius of curvature, roughly that of the earth. This problem has been solved in general only for a smooth dielectric or conducting sphere.

In the sections that follow we examine several specialized propagation models: (1) propagation over a plane, (2) propagation over a knife-edge on a plane, and (3) propagation over a smooth spherical earth. The solutions to these problems give some insight into the problems of propagation modeling.

6.2 Propagation Over a Plane

The standard method of investigating propagation over a flat plane makes use of the fact that the plane reflects like a mirror, and the reflected wave can be assumed to originate at the mirror image of the source. In effect, one replaces the reflecting plane by the image of the source and assigns a phase shift to the image wave to take into account the phase change upon reflection. Also, the amplitude of the reflected wave must be multiplied by a factor equal to the magnitude of the reflection coefficient. The direct wave and the wave from the image combine to form a pattern of lobes and nulls. Figure 6.1 shows the geometry of the problem. If the horizontal distance to the target is large compared with the heights z_1 and z_2, then the path difference is:

$$\Delta R = d_2 - d_1 = 2 \, z_1 \, z_2 / x$$

Let us assume that the source is a radar with the axis of its antenna beam pointed horizontally toward the target and that the pattern of the antenna is

42
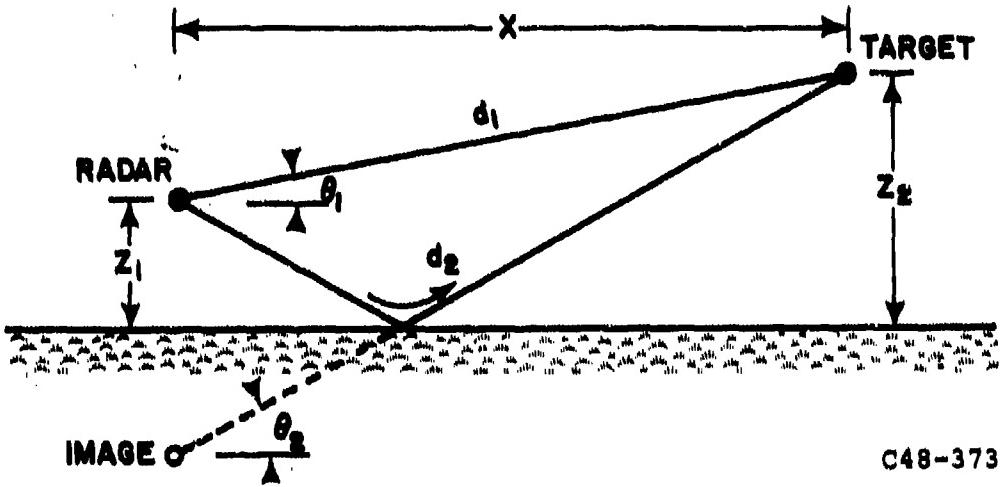
Fig. 6.1 Diagram of propagation over a plane.

C48-373

given by $f(\theta)$, where θ is the angle between the horizontal and the target viewed from the radar antenna or from the mirror image of the antenna. Then the pattern propagation factor will be given by:

$$F = |f(\theta_1) + \rho f(\theta_2) \, e^{-i(2\pi \, \Delta R/\lambda + \phi)}|$$

where: R = range from radar to target,

θ_1 = $(z_2 - z_1)/R$ (radians),

θ_2 = $(z_2 + z_1)/R$ (radians),

$\rho e^{-i\phi}$ = complex reflection coefficient,

λ = wavelength.

Since the phase shift will normally be π at low elevation angles (see Section 4.2), nulls will be produced when the target height has values:

$$z_2 = 0, \; \left(\frac{\lambda x}{2z_1}\right), \; 2\left(\frac{\lambda x}{2z_1}\right), \; 3\left(\frac{\lambda x}{2z_1}\right) \; \ldots$$

and peaks produced for target heights

$$z_2 = \frac{\lambda x}{4z_1}, \; 2\left(\frac{\lambda x}{4z_1}\right), \; 3\left(\frac{\lambda x}{4z_1}\right) \; \ldots$$

The widths of the lobes are thus directly proportional to wavelength and inversely proportional to radar-antenna height.

If we neglect the antenna pattern, then the ratio of the null signal strength to the peak signal strength, expressed in decibels, is 20 log $(1-\rho)/(1+\rho)$. For example, the null-to-peak power ratios are -15 dB for $\rho = 0.7$, -9.5 dB for $\rho = 0.5$, and -5.4 dB for $\rho = 0.3$. A standard method for measuring reflection coefficient makes use of the relationship between null-to-peak ratios and reflection coefficient.

6.3 Propagation Over a Knife-Edge on a Plane

The problem of propagation over a flat plane can be generalized to include a knife-edge mask on the plane. This is accomplished by using images

44

to represent the reflected waves. Since reflections may occur on both sides of the knife-edge, images of both the radar and the target must be considered. Figure 6.2 shows the ray paths; Figure 6.2(a) represents paths with reflections and Figure 6.2(b) represents equivalent paths by the method of images. Four separate paths must be taken into account, and this is sometimes referred to as the four-ray problem. A program has been written to solve this problem when the dimensions are specified and the reflection coefficients given for the plane on each side of the mask. A complete description of this program, with a program listing, is given in Appendix A.

We have calculated the pattern propagation factor with this program for a representative situation: the target range 15 km, the mask 10 km from the radar, and both the radar and the edge of the mask are 100 m above the reflecting plane. For each radar frequency, four cases are worked out; the one-way propagation loss relative to free space (20 log F) is calculated for a range of target heights 0 to 250 m, (1) with $\rho = 0$ on both sides of the mask, (2) for reflection on the left side only, (3) for reflections on the right side only, and (4) for reflections on both sides. These four cases are shown for an L-band radar frequency (1.3 GHz) in Figure 6.3. When ρ(left) and ρ(right) are both zero we get the familiar Fresnel diffraction curve. When reflection occurs on the left only, we get a hybrid situation with lobe structure above 200 m where the direct and reflected waves interfere, and diffraction of both waves into the shadow zone with little change in their relative phase. When reflection occurs on the right only, we find interference lobing between the direct and reflected wave with increasingly deep nulls as the target moves into the shadow zone. We can think of the knife-edge as the source of the diffracted wave in the shadow zone, and the lobe width is determined by the height of the knife-edge above the reflecting plane. When reflection occurs on both sides of the mask, the propagation combines the characteristics of the two cases of single reflection.

A similar computation made for a VHF frequency (170 MHz) is shown in Figure 6.4; the geometrical arrangement is identical to that of Figure 6.3.

45
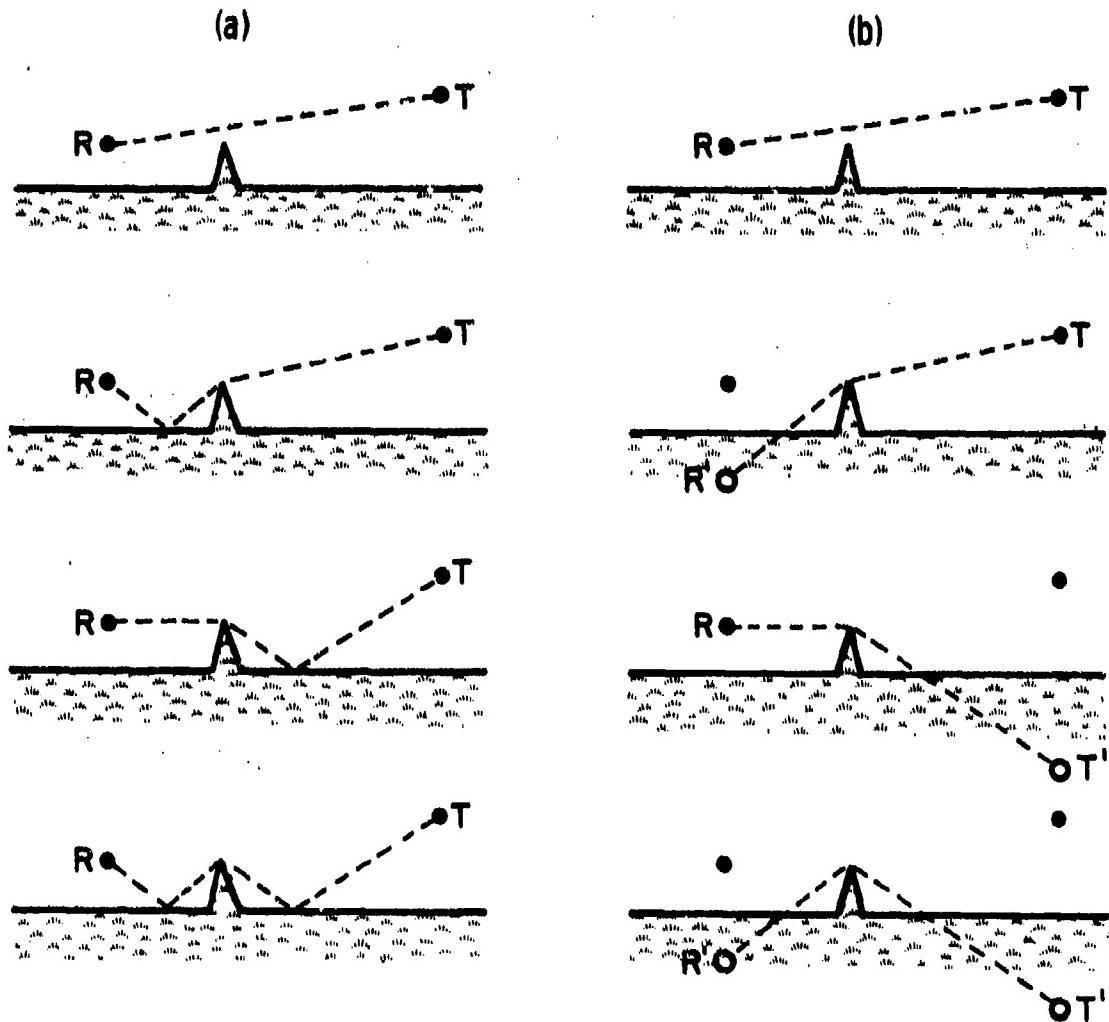
Fig. 6.2 Diagram of the four-ray problem. (a) shows the direct and reflected rays and (b) the equivalent construction with images.
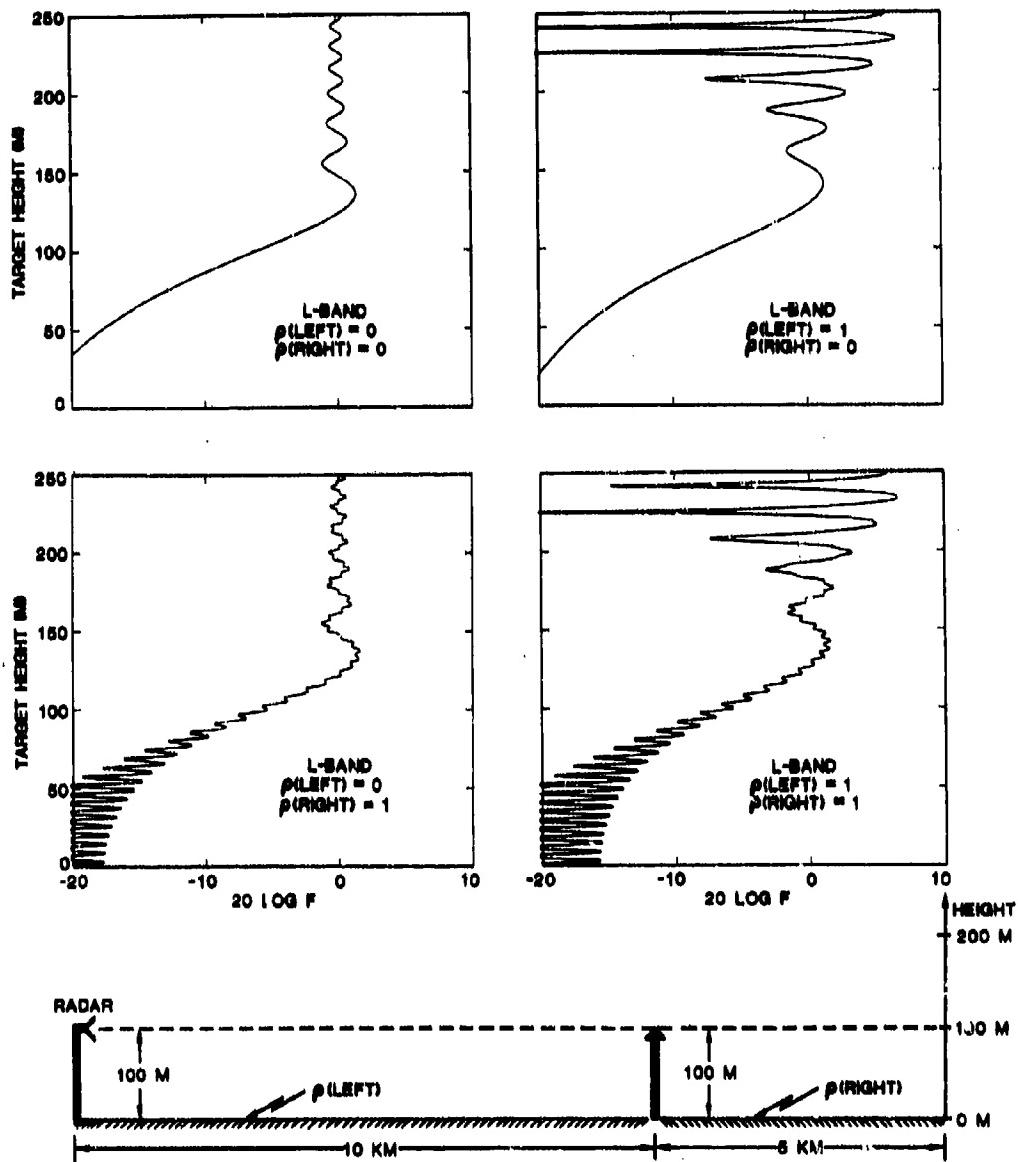
Fig. 6.3 Propagation over a knife-edge on a plane at a frequency of 1.3 GHz. The propagation geometry is shown in the bottom diagram; the four graphs show the cases of perfect reflection or no reflection on each side of the knife-edge.
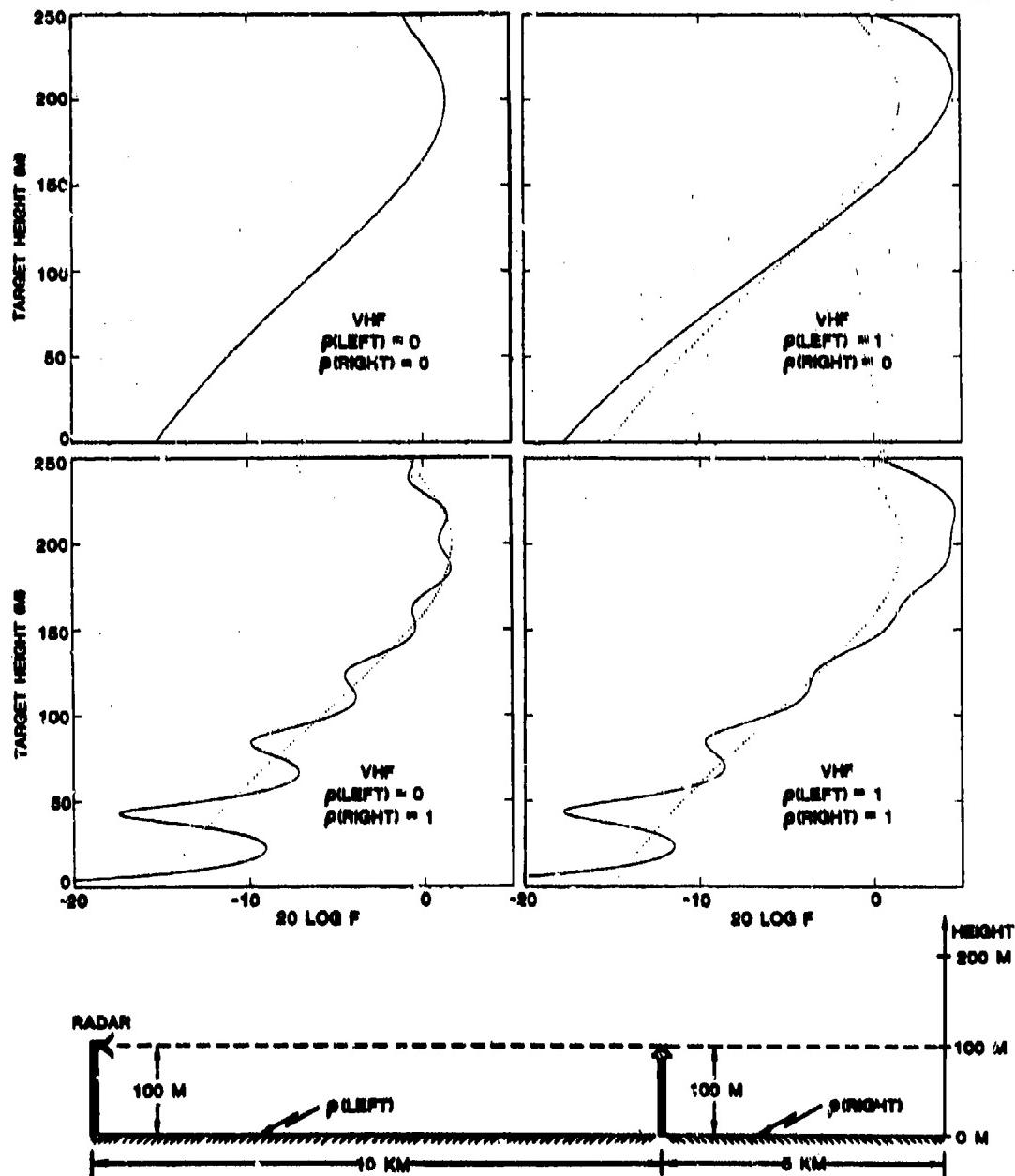
Fig. 6.4 Propagation over a knife-edge in a plane at a frequency of 170 MHz. The propagation geometry is identical with that of Fig. 6.3. The dotted line shows the curve with no reflection for comparison.

The target-height scale for this radar frequency goes only up to 250 m, not high enough to show the lobe pattern which is produced by reflections in the foreground of the radar. With reflections only on the left side of the mask, the signal strength is increased for heights from 150 to 250 m and decreased for heights below 100 m as compared to the diffraction-only case. With reflections on the target side of the mask, one finds lobes in the shadow zone which result from interference between waves from the virtual source at the knife-edge as in the L-band case. The dotted curves in Figure 6.4 represent the diffraction-only case for comparison.

6.4 Propagation Over a Spherical Earth

The problem of radio propagation over a smooth spherical earth is discussed in detail by KERR (1951), by Domb and Price (1946), and by many others. We describe here the solution of this classical problem; the references cited above should be consulted for a complete discussion of the problem. The radius of the sphere is, of course, taken to be the effective earth radius, i.e., radius of curvature of the terrain profile corrected for atmospheric refraction. For a radar antenna at height h_1, the range r_1 to the horizon is given by $\sqrt{2h_1 K R_e}$, and looking from the target toward the radar, the range r_2 to the horizon is $\sqrt{2h_2 K R_e}$, where h_2 is the target height. Hence, the range r at which the line-of-sight from radar to target is just tangent to the earth (i.e., the lowest line-of-sight) is given by:

$$r_1 + r_2 = \sqrt{2 h_1 K R_e} + \sqrt{2h_2 K R_e}$$

These results may be derived from simple geometrical considerations.

The solution to the problem will be considered in three separate regions. Figure 6.5 shows how these regions are defined in terms of the lowest line-of-sight. In the interference region the propagation is determined by the interference of the direct and reflected waves. The path difference is computed from geometrical considerations and the amplitude of the reflected wave is corrected for the increased divergence of the rays produced by

C48-374
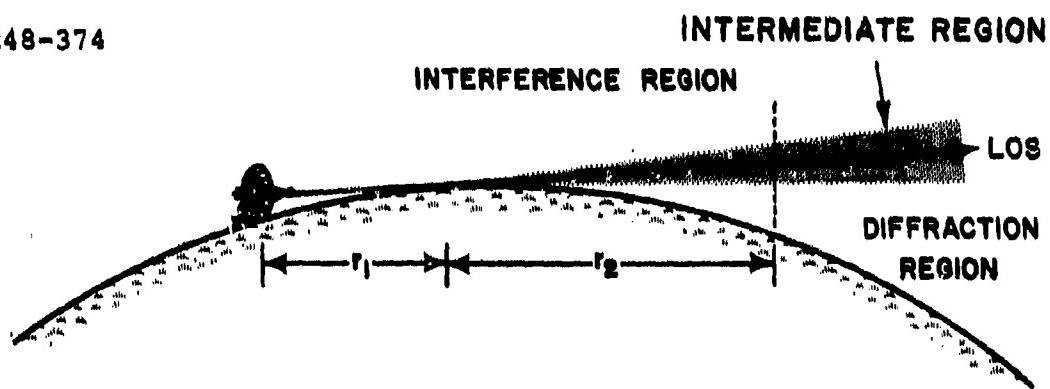
Fig. 6.5 Propagation regions over a smooth spherical earth.

reflection from a convex surface. The boundary of the interference region may be taken as the line along which the path difference for the direct and reflected waves equals $\lambda/8$. The diffraction region includes points that lie sufficiently far below the tangent ray for the field to be represented by a single mode; in the intermediate region all modes (the complete residual-series solution) are required to describe the field. Domb and Price (1946) give a convenient method for obtaining the pattern propagation factor along the tangent ray and within the diffraction region.

We have programmed the interference-region computations of the pattern propagation function $\underline{F}$; a description of this program is contained in Appendix B. As an example of this calculation, we show in Figure 6.6 the distributions of values of $\underline{F}$, at various ranges, for a transmitting antenna at a height of 30 m above a smooth spherical earth (reflection coefficient = 0.9 and K = 4/3) calculated for wavelength λ = 23 cm. We see the characteristic lobe structure represented in this plot. Note that the lobes and peaks line up along a straight line in Fig. 6.6. The lower boundary of the interference region, where the path difference of the direct and reflected wave equals $\lambda/8$, also lies along a straight line in Fig. 6.6. The figure shows values of F which vary between 1.9 (peaks) and 0.1 (nulls). The pattern of the transmitting antenna is assumed to effectively cut off the signal in the upper left corner.

For low-flying aircraft we must consider propagation loss below the interference region. Figure 6.7 shows plots of F vs. altitude for a target range of 30 km and an antenna height of 30 m. The lowest line-of-sight corresponds to a target height of 3.25 m. For this figure we assumed ρ = 0.7 and K = 4/3; the wavelengths represent VHF (λ = 200 cm), L-band (λ = 23 cm), and X-band (λ = 3.3 cm). The boundary of the interference region is indicated for each wavelength. The boundary is at the following target heights: 170 m for λ = 200 cm, 39 m for λ = 23 cm, and 15 m for λ = 3.3 cm. For the range of altitudes in Figure 6.7, almost the entire curve for VHF wavelengths lies in the intermediate region, while at X-band most of the curve lies in the interference region. Note that the depths of the nulls in the X-band curve decrease as the altitude decreases. This is a consequence of the divergence factor mentioned
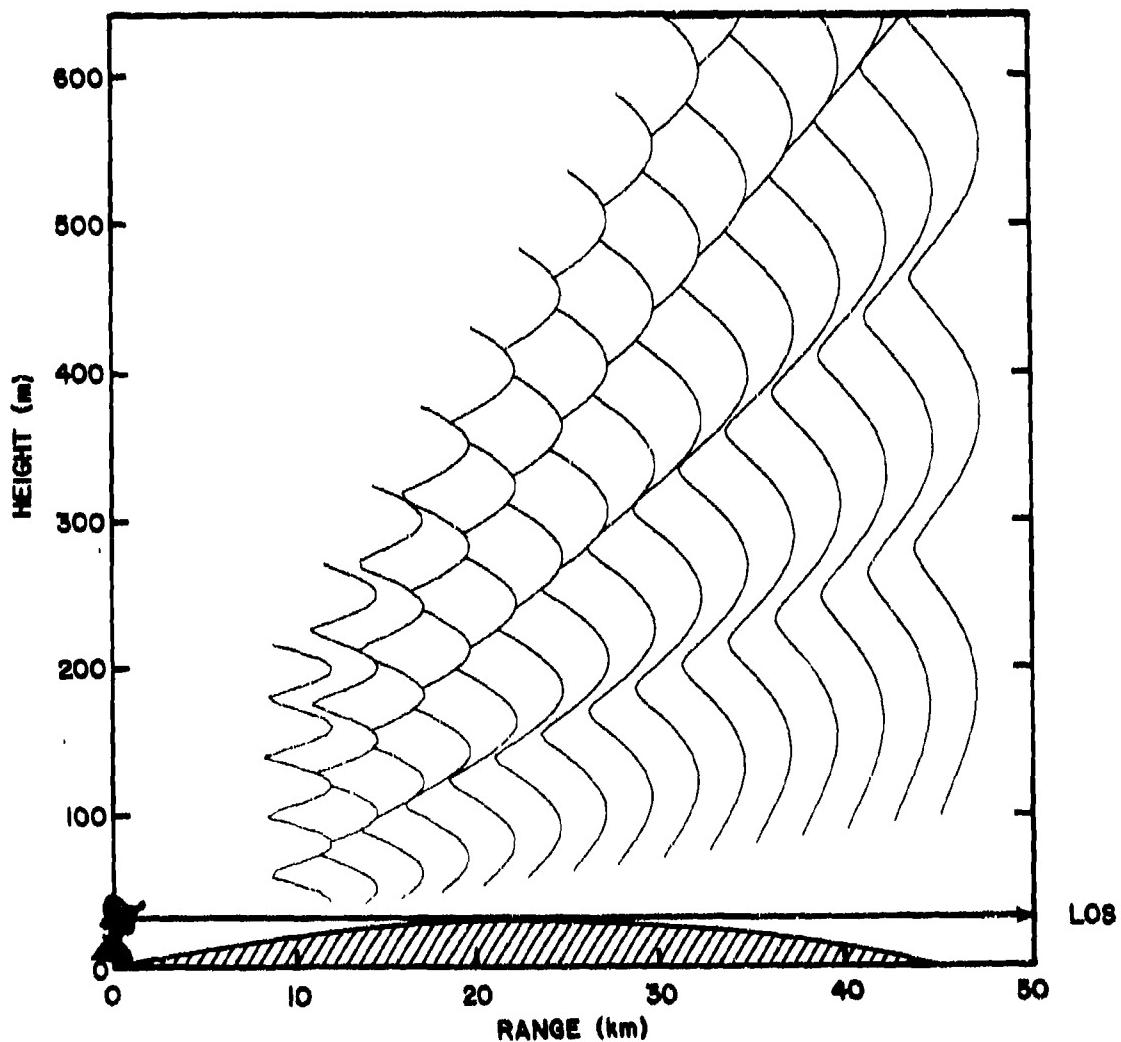
Fig. 6.6 The space distribution of the pattern propagation function for the interference region over a spherical earth. Parameters are given in the text.
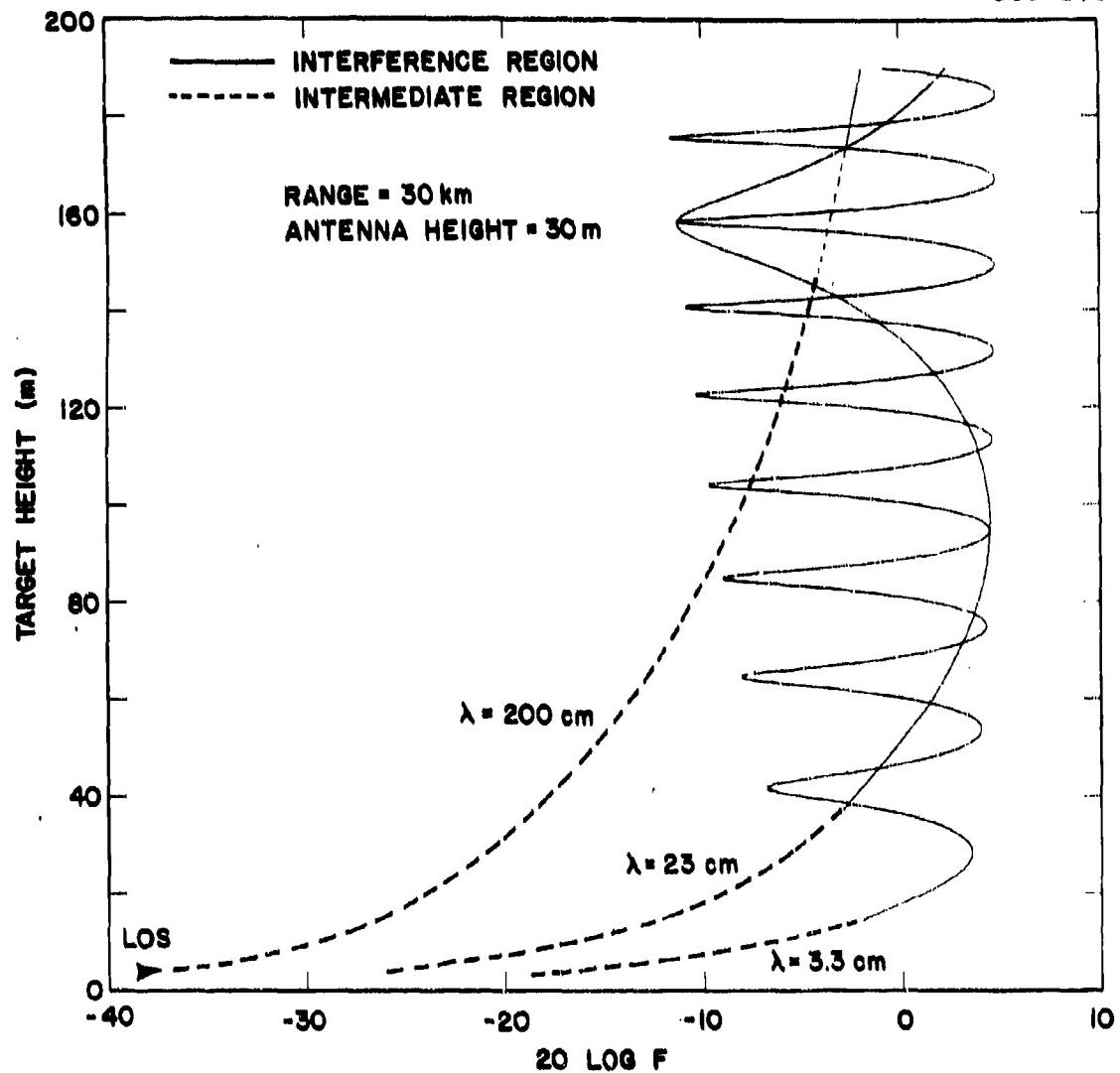
Fig. 6.7 The pattern propagation function vs. target altitude in the inter-
ference region and below. Three wavelengths are represented: 3.3, 23 and 200 cm;
the $\lambda/8$ boundary of the interference region is indicated for each wavelength by
the change from solid to dotted line. The lowest line-of-sight corresponds to
a target height of 3.25 m.

earlier. As a result of diffraction by a smooth spherical earth, we expect that the VHF wavelengths will suffer a much greater propagation loss than shorter L-band and X-band wavelengths for very low-flying targets. These predictions, however, apply to propagation over a highly reflective earth; for example, over a calm sea. We know of no complete solution for the interference region that specifically includes the effect of surface roughness, but in the interference region one can, in principle, take roughness into account by assigning a reflection coefficient. In the spherical-earth program described in Appendix B, the reflection coefficient is represented by a parameter that may be specified.

7. SUMMARY

Low-altitude propagation at frequencies above 100 MHz is controlled by atmospheric refraction and by diffraction and reflection from the terrain over which the waves travel. Where these phenomena can be taken into account quantitatively, we can predict accurately the propagation loss as a function of frequency over specific terrain. The underlying physical principles are understood, but a number of difficulties remain before the low-altitude-propagation problem can be considered solved.

Refraction plays an important role in the propagation of radar waves over large bodies of water, particularly over the ocean in lower altitudes. Electromagnetic waves may be trapped in surface layers of air containing a concentration of water vapor and an inversion of the temperature gradient. Greatly extended radar ranges in such ducts are encountered frequently in maritime environments. On the other hand, over continental land masses ducting is infrequent. Nevertheless, over areas of desert or snow cover, nocturnal temperature inversions due to radiational cooling may significantly affect propagation. But usually the atmosphere near the surface over land has a refractivity that decreases nearly linearly with increasing altitude. This situation, encountered roughtly 80 percent of the time, can be modeled by increasing the effective earth radius by a factor which varies between one and two, a typical value being 4/3. Taking refraction into account is straightforward in this case,

and the resulting effect on radar coverage is comparatively small and independent of radar frequency.

Diffraction phenomena on the other hand are of major importance in low-altitude propagation, and we must distinguish between two cases. In the first case specific irregularities in the terrain profile produce diffraction; these terrain features can be represented by knife-edges, or in some cases by cylinders. In the second case diffraction is produced by the curvature of the smooth spherical earth, and this case applies to propagation over oceans or very smooth plains. In both cases the propagation is strongly dependent on radar frequency; the boundary between the illuminated region and the shadow becomes increasingly sharp as the frequency increases. At lower frequencies diffraction by hills or ridges alters the field strength in a significant region above and below the lowest line of sight. Diffraction reduces the signal above the mask and at the same time directs some energy into the shadow region below the mask. Consequently, at lower frequencies several diffracting features in the terrain profile will usually contribute to the propagation loss. This presents a problem that has yet to be completely solved: we lack an adequate model for more than two knife-edges in series. Furthermore, we do not know the extent to which the rigorous solution to the problem of propagation over a smooth spherical earth is applicable when the terrain is not perfectly smooth. These problems require thorough investigation. For example, we should be able to specify the conditions under which the multiple-diffraction case goes over to the spherical earth case as the terrain roughness decreases.

The effect of coherent reflection from terrain must be taken into account for propagation paths over water and smooth plains, particularly at lower frequencies. The lobe structure produced by reflections from a plane gives a null at the horizon, and the depth of this null depends on the reflection coefficient. So coherent reflection from terrain can alter low-altitude propagation significantly depending on the value of the reflection coefficient. If the terrain is perfectly smooth, the conductivity and dielectric constant of the surface determine the reflection coefficient, but for real terrain the roughness must

be taken into account. For barren terrain the Gaussian terrain model may be used to estimate the effect of terrain irregularity, but this model has not been verified for very low grazing angles. Furthermore, the reflection properties of terrain with vegetative cover are almost unknown for grazing angles below one degree. Thus, extensive measurements over barren and vegetated terrain must be made to develop a valid model for reflection effects.

The standard models of propagation described here involve: (1) propagation over a plane with arbitrary reflection coefficient, (2) propagation over a sphere in a region above the horizon where the direct and reflected waves interfere, (3) propagation over a knife-edge on a reflecting plane, and (4) propagation over successive knife-edges treated approximately by the method of Deygout (1966). In many cases these models are adequate for predicting propagation loss provided the reflection coefficients are known.

APPENDIX A

FOUR-RAY PROPAGATION MODEL

This model calculates the pattern propagation factor F for radio propa-
gation over flat terrain on which a knife-edge obstruction lies perpendicular
to the direction of propagation. The geometrical arrangement is shown in
Fig. A-   program computes F for a sequence of values of Z_2, the height of
R above

Input	Output
Geometrical distances in meters: Z_1, d_1, d_2, f, and the initial value, final value, and step for Z_2.	Table with the following columns: Height of R: Z_2 (in meters), F (pattern propagation factor), and 20 log F.
Wavelength λ in meters	For Rays 1 and 2: v, $\|E\|$, ρ_1,
Polarization: Horizontal (H) or Vertical (V)	ϕ_1 and v_2, $\|E_2\|$, ρ_2, ϕ_2
	For Ray 4: v_4 and $\|E_4\|$

Ground properties on left and right
   side of the mask: Relative dielectric
   constant ϵ, conductivity σ (in mhos/m)

(Note: The reflection coefficient on
   either or both sides may be taken
   as zero if $\epsilon = \sigma = 888$.)

In case the surface is rough, the re-
   flection coefficient may be altered
   by factors REF L and REF R on the left
   and right sides of the mask.

Reflections on the left and right sides are taken into account by including the
images of R and T which are denoted by S and U, respectively. The four possible
rays to be considered are TR, UR, TS, and US, which are designated as Rays 1, 2,

57

C48-379
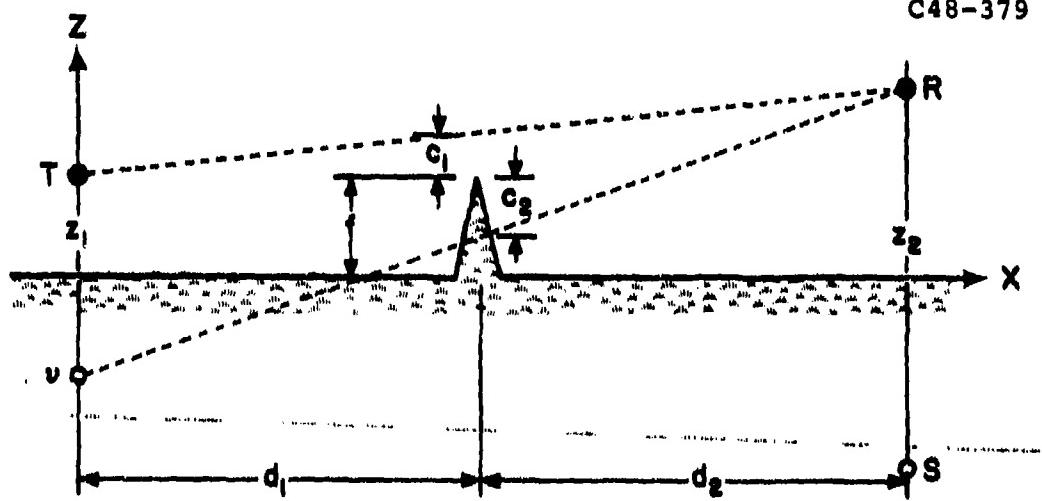
Fig. A-1 Geometrical arrangement in the four-ray model.

3, and 4, respectively. The reflection coefficients are designated by the subscripts 1 and 2 for the left and right sides, respectively. Each reflection coefficient Γ is given by a complex number calculated from the Fresnel reflection formulas in a subroutine, FRESNL, and Γ has the form

$$\Gamma = \rho e^{-i\phi}$$

where the magnitude ρ and the phase lag ϕ depend on the grazing angle, the polarization, and the electrical constants, ε and σ, of the ground. The Fresnel integrals $C(v)$ and $S(v)$, are evaluated in a subroutine, DCS, where $v = \sqrt{2}\ c$ with c equal to the ray clearance over the knife-edge. (When the ray intersects the mask, c is taken as negative.) The pattern propagation factor is equal to $|F|$, where

$$F = \sum_{k=1}^{4} E_k \exp{(i\psi)}$$

and

$$E_1 = A_1 \qquad\qquad \psi_1 = \beta_1$$

$$E_2 = \Gamma_1 A_2 \qquad\qquad \psi_2 = \beta_2 + \frac{2\pi}{\lambda}(R_1 - R_2)$$

$$E_3 = \Gamma_2 A_3 \qquad\qquad \psi_3 = \beta_3 + \frac{2\pi}{\lambda}(R_3 - R_1)$$

$$E_4 = \Gamma_1 \Gamma_2 A_4 \qquad\qquad \psi_4 = \beta_4 + \frac{2\pi}{\lambda}(R_4 - R_1)$$

$$A = \frac{1}{\sqrt{2}}\ [(C(v) + 1/2)^2 + (S(v) + 1/2)^2]^{1/2}$$

$$\beta = \tan^{-1}\left(\frac{S + 1/2}{C + 1/2}\right) - \pi/4 \text{ if } (C + 1/2) \geq 0$$

$$\beta = \pi + \tan^{-1}\left(\frac{S + 1/2}{C + 1/2}\right) - \pi/4 \text{ if } (C + 1/2) < 0$$

This computation was programmed in IBM FORTRAN IV ANSI by Gerald McCaffrey; a copy of the listings for this program as well as a sample of the output follow this description. The sample computation appears plotted as Fig. 6.4, and all the input parameters are listed on the output.

PROGRAM LISTINGS · FOUR-RAY PROPAGATION MODEL

PROGRAMMED BY GERALD McCAFFREY

```
C
C      VARIABLES THAT START WITH THE LETTER C ARE COMPLEX
C
       COMPLEX CT1,CT2,CF,CE1,CE2,CE3,CF4,CTH,CTV
       REAL*8 R1,R2,R3,R4,VC1,VC2,VC3,VC4,VS1,VS2,VS3,VS4,A,B,V1,V2,V3,V4
       REAL*8 VTERM
       REAL*4 LAMDA
       DIMENSION POLAR(2)
       DATA POLAR/'H    ','V    '/
       PI=3.14159
       RAD=57.29578
C
C   GET SQRT(2.0)
C
       SQRT2=SQRT(2.0)
C
C   READ GEOMETRIC PARAMETERS
C
       WRITE(6,1)
1      FORMAT(' INPUT Z1,D1,D2,F,Z2S,Z2E,DZ2')
       READ(5,*) Z1,D1,D2,F,Z2S,Z2E,DZ2
C
C   READ IN DIALECTIC CONSTANTS AND FRESNEL FACTORS (LEFT AND RIGHT)
C
       WRITE(6,4)
4      FORMAT(' INPUT PSIL,SL,PSIR,SR,REFL,REFR')
       READ(5,*) EL,SL,ER,SR,REFL,REFR
C
C   READ IN POLARIZATION
C
       WRITE(6,2)
2      FORMAT(' INPUT POLARIZATION.. H=HORIZONTAL,V=VERTICAL')
       READ(5,3) POLR
3      FORMAT(A4)
       IF(POLR.EQ.POLAR(1)) IPOL=1
       IF(POLR.EQ.POLAR(2)) IPOL=2
C
C   INITIALIZE Z2
C
       Z2=Z2S-DZ2
C
C   SET WAVELENGTH
C
```

```
          LAMDA=.302
C
C      WRITE OUT THE INPUTS AND SET UP HEADER FOR THE PRINTOUT
C
       WRITE(1,10) Z1,D1,D2,F,Z2S,Z2E,DZ2,LAMDA,POLR,EL,ER,SL,SR
       WRITE(1,9)
9      FORMAT(' ')
       WRITE(6,10) Z1,D1,D2,F,Z2S,Z2E,DZ2,LAMDA,POLR,EL,ER,SL,SR
      1,REFL,REFR
10     FORMAT(' ANNT HT',F6.2,' D1',F6.0,' D2',F6.0,' F',F6.1,15X,
      1' TARGET HT FROM',F5.0,' TO',F5.0,' BY',F5.0,/' WAVELENGTH',F6.3,
      3' POLARIZATION ',A4,' EPSILON L',F8.3,' EPSILON R',F8.3,' SIG L',
      4F8.3,' SIG R',F8.3/,' REFL',F10.2,' REFR',F10.2)
       WRITE(1,11)
11     FORMAT(2X,'TARGET HT',2X,' F ',1X,'20LOG(F)',1X,' V(1)',1X,
      1' MAG(E1)',2X,' RHO(1)',1X,' PHI(1)',1X,' V(2)',1X,' MAG(E2)',3X,
      2' V(3)',1X,' MAG(E3)',1X,' RHO(2)',1X,' PHI(2)',3X,' V(4)',1X,
      3' MAG(E4)')
C
C      CALCULATE HO
C
       HO1=LAMDA*D1*D2
       HO2=D1+D2
       HO=SQRT(HO1/HO2)
C
C      LOOP ON Z2 FROM Z2S TO Z2E BY DZ2
C
100    Z2=Z2+DZ2
       IF(Z2.GT.Z2E) GO TO 1000
C
C      CALCULATE R1,R2,R3,AND R4
C
       R1=DSQRT((Z2*1.0D0-Z1)**2+(D1+D2)**2)
       R2=DSQRT((-Z2*1.0D0-Z1)**2+(D1+D2)**2)
       R3=R2
       R4=R1
C
C      CALCULAT V1,V2,V3,AND V4
C
       VTERM=((Z2*1.0D0-Z1)*D1)/(D1+D2)
       V1=SQRT2/HO*(Z1+VTERM-F)
C
       VTERM=((Z2*1.0D0+Z1)*D1)/(D1+D2)
       V2=SQRT2/HO*(-Z1+VTERM-F)
C
       VTERM=((-Z1*1.0D0-Z2)*D1)/(D1+D2)
       V3=SQRT2/HO*(Z1+VTERM-F)
C
       VTERM=((Z1*1.0D0-Z2)*D1)/(D1+D2)
       V4=SQRT2/HO*(-Z1+VTERM-F)
C
C      CALCULATE THE GRAZING ANGLES
```

```
C
C       LEFT GRAZING ANGLE
C
      IF(V2.GE.0) GO TO 200
C
C      RAY INTERSECTS MASK
C
      PSIL=DATAN((Z1+F)/D1*1.0D0)
      GO TO 201
C
C      RAY CLEAR OF MASK
C
200   PSIL=DATAN((Z2+Z1)/(D1+D2*1.0D0))
C
C       RIGHT GRAZING ANGLE
C
201   IF(V3.GE.0) GO TO 205
C
C      RAY INTERSECTS MASK
C
      PSIR=DATAN((Z2+F)/D2*1.0D0)
      GO TO 206
C
C      RAY CLEAR OF MASK
C .
205   PSIR=DATAN((Z2+Z1)/(D1+D2*1.0D0))
C
C      CALL THE COMPLEX REFLECTION COEFFICIENT SUBROUTINE
C
C      FOR THE LEFT
C
206   CALL FRESNL(EL,LAMDA,SL,PSIL,CTH,CTV)
C
C      MULTIPLY BY FACTORS
C
      CTH=CTH*REFL
      CTV=CTV*REFL
C
C      SET CT1
C
      IF(IPOL.EQ.1) CT1=CTH
      IF(IPOL.EQ.2) CT1=CTV
C
C      888 SHOWS NO REFLECTION ON THE LEFT
C
      IF(EL.EQ.888.AND.SL.EQ.888) CT1=CMPLX(0.0,0.0)
C
C      FOR THE RIGHT
C
      CALL FRESNL(ER,LAMDA,SR,PSIR,CTH,CTV)
C
C      MULTIPLY BY FACTORS
```

62

```
C
        CTH=CTH*REFR
        CTV=CTV*REFR
C
C     SET CT2
C
      IF(IPOL.EQ.1) CT2=CTH
        IF(IPOL.EQ.2) CT2=CTV
C
C     888 SHOWS NO REFLECTION ON THE RIGHT
C
        IF(ER.EQ.888.AND.SR.EQ.888) CT2=CMPLX(0.0,0.0)
C
C     GET THE REAL AND IMAGINARY PARTS FOR VERT AND HORZ
C
        P1R=REAL(CT1)
        P1I=AIMAG(CT1)
        P2R=REAL(CT2)
        P2I=AIMAG(CT2)
C
C     GET THE PHASE LAG IN DEGREES
C
        THETA1=0
        THETA2=0
      IF(P1I.NE.0.AND.P1R.NE.0)THETA1=ATAN2(P1I,P1R)*(-RAD)
        IF(P2I.NE.0.AND.P2R.NE.0)THETA2=ATAN2(P2I,P2R)*(-RAD)
C
C     GET THE REFLECTION COEF
C
        PR1=CABS(CT1)
        PR2=CABS(CT2)
C
C     CALCULATE COMPLEX F (CF)
C       BY FIRST CALCULATING THE COMPLEX PARTS CE1,CE2,CE3,AND CE4
C
C     CALCULATE CE1 USING V1
C
        CALL DCS(VC1,VS1,V1)
        A=1/SQRT2*DSQRT((VC1+0.5)**2+(VS1+0.5)**2)
        IF(VC1+0.5.GE.0) B=DATAN((VS1+0.5)/(VC1+0.5))-PI/4
        IF(VC1+0.5.LT.0) B=PI+DATAN((VS1+0.5)/(VC1+0.5))-PI/4
        A1=A*DSIN(B)
        B1=A*DCOS(B)
        CE1=CMPLX(B1,A1)
C
C     CALCULATE CE2 USING V2
C
        CALL DCS(VC2,VS2,V2)
        A=1/SQRT2*DSQRT((VC2+0.5)**2+(VS2+0.5)**2)
        IF(VC2+0.5.GE.0) B=DATAN((VS2+0.5)/(VC2+0.5))-PI/4
        IF(VC2+0.5.LT.0) B=PI+DATAN((VS2+0.5)/(VC2+0.5))-PI/4
        B=B+(2*PI)/LAMDA*(R2-R1)
```

63

```
      A1=A*DSIN(B)
      B1=A*DCOS(B)
      CE2=CMPLX(B1,A1)*CT1
C
C     CALCULATE CE3 USING V3
C
      CALL DCS(VC3,VS3,V3)
      A=1/SQRT2*DSQRT((VC3+0.5)**2+(VS3+0.5)**2)
      IF(VC3+0.5.GE.0) B=DATAN((VS3+0.5)/(VC3+0.5))-PI/4
      IF(VC3+0.5.LT.0) B=PI+DATAN((VS3+0.5)/(VC3+0.5))-PI/4
      B=B+(2*PI)/LAMDA*(R3-R1)
      A1=A*DSIN(B)
      B1=A*DCOS(B)
      CE3=CMPLX(B1,A1)*CT2
C
C     CALCULATE CE4 USING V4
C
      CALL DCS(VC4,VS4,V4)
      A=1/SQRT2*DSQRT((VC4+0.5)**2+(VS4+0.5)**2)
      IF(VC4+0.5.GE.0) B=DATAN((VS4+0.5)/(VC4+0.5))-PI/4
      IF(VC4+0.5.LT.0) B=PI+DATAN((VS4+0.5)/(VC4+0.5))-PI/4
      A1=A*DSIN(B)
      B1=A*DCOS(B)
      CE4=CT1*CT2*CMPLX(B1,A1)
C
C     NOW ADD TO GET CF
C
      CF=CE1+CE2+CE3+CE4
C
C     WRITE OUT ANSWERS
C
      FO=CABS(CF)
      FLOG=20*ALOG10(FO)
      E1MAG=CABS(CE1)
      E2MAG=CABS(CE2)
      E3MAG=CABS(CE3)
      E4MAG=CABS(CE4)
      WRITE(1,99) Z2,FO,FLOG,V1,E1MAG,PR1,THETA1,V2,E2MAG,V3,E3MAG,
     1PR2,THETA2,V4,E4MAG
99    FORMAT(F8.1,4(2F7.2,F10.3),2F8.2)
      GO TO 100
1000  RETURN
      END
```

SUBROUTINE FOR COMPLEX REFLECTION COEFFICIENTS

```
      SUBROUTINE FRESNL(El,WAVE,CONDUC,ANG,CTH,CTV)
      COMPLEX CAK,CTV,CTV1,CTV2,CTH,CTH1,CTH2
C
C       El.......THE DIELECTIC CONSTATNT (FROM 0 TO 100)
C       LAMDA....THE WAVELENGTH IN METERS
C       CONDUC...THE CONDUCTIVITY IN MHOS/METER
C       ANG......THE ANGLE IN RADIANS
C
C
C       CALCULATE THE COMPLEX CONSTANT
C
      AKI=-60*WAVE*CONDUC
      CAK=CMPLX(El,AKI)
C
C       CALCULATE THE VERTICAL POLARIZATION
C
      CTV1=CAK*SIN(ANG)-CSQRT(CAK-COS(ANG)**2)
      CTV2=CAK*SIN(ANG)+CSQRT(CAK-COS(ANG)**2)
      CTV=CTV1/CTV2
C
C       CALCULATE THE HORIZONTAL
C
      CTH1=SIN(ANG)-CSQRT(CAK-COS(ANG)**2)
      CTH2=SIN(ANG)+CSQRT(CAK-COS(ANG)**2)
      CTH=CTH1/CTH2
1000  RETURN
      END
```

SUBROUTINE TO EVALUATE THE FRESNEL INTEGRALS

```
      SUBROUTINE DCS (C,S,X)
      IMPLICIT REAL*8 (A-H,O-Z)
      DIMENSION CC(12),DD(12),AA(12),BB(12)
      U=X
      PIB2=1.5707963268D0
      X=PIB2*X*X
      Z=DABS(X)
      IF(Z.NE. 0.D0) GO TO 1000
      C=0.D0
      S=0.D0
      X=U
      RETURN
1000  CONTINUE
      IF(Z-4.0D0)3,3,4
  3   C=DCOS(Z)
      S=DSIN(Z)
      Z=Z/4.0D0
      DZ=DSQRT(Z)
```

65

```fortran
      AA(1)=0.159576914D+01
      AA(2)=-0.1702D-05
      AA(3)=-0.6808568854D+01
      AA(4)=-0.576361D-03
      AA(5)=0.6920691902D+01
      AA(6)=-0.16898657D-01
      AA(7)=-0.305048566D+01
      AA(8)=-0.75752419D-01
      AA(9)=0.850663781D0
      AA(10)=-0.25639041D-01
      AA(11)=-0.15023096D0
      AA(12)=0.34404779D-01
      BB(1)=-0.33D-07
      BB(2)=0.4255387524D+01
      BB(3)=-0.9281D-04
      BB(4)=-0.77800204D+01
      BB(5)=-0.9520895D-02
      BB(6)=0.5075161298D+01
      BB(7)=-0.138341947D0
      BB(8)=-0.1363729124D+01
      BB(9)=-0.403349276D0
      BB(10)=0.702222016D0
      BB(11)=-0.216195929D0
      BB(12)=0.19547031D-01
      ASUM=AA(1)
      BSUM=BB(1)
      DO 40 J=2,12
      ASUM=ASUM+AA(J)*Z**(J-1)
      BSUM=BSUM+BB(J)*Z**(J-1)
40    CONTINUE
      FC=DZ*(S*BSUM+C*ASUM)
      FS=DZ*(-C*BSUM+S*ASUM)
      C=FC
      S=FS
      GO TO 5
4     D=DCOS(Z)
      S=DSIN(Z)
      Z=4.0D0/Z
      CC(1)=0.0D0
      CC(2)=-0.24933957D-01
      CC(3)=0.3936D-05
      CC(4)=0.5770956D-02
      CC(5)=0.689892D-03
      CC(6)=-0.9497136D-02
      CC(7)=0.11948809D-01
      CC(8)=-0.6748873D-02
      CC(9)=0.24642D-03
      CC(10)=0.2102967D-02
      CC(11)=-0.121793D-02
      CC(12)=0.233939D-03
      DD(1)=0.19947114D0
      DD(2)=0.23D-07
```

66

```
        DD(3)=-0.9351341D-02
        DD(4)=0.23006D-04
        DD(5)=0.485146D-02
        DD(6)=0.1903218D-02
        DD(7)=-0.17122914D-01
        DD(8)=0.29064067D-01
        DD(9)=-0.27928955D-01
        DD(10)=0.16497308D-01
        DD(11)=-0.5598515D-02
        DD(12)=0.838386D-03
        DSUM=DD(1)
        CSUM=CC(1)
        DO 30 J=2,12
        CSUM=CSUM+CC(J)*Z**(J-1)
   30   DSUM=DSUM+DD(J)*Z**(J-1)
        Z=DSQRT(Z)
        C=0.5D0+Z*(D*CSUM+S*DSUM)
        S=0.5D0+Z*(S*CSUM-D*DSUM)
   5    X=U
        IF(U.GT.0.D0) GO TO 6
        C=-C
        S=-S
   6    RETURN
        END
```

SAMPLE OUTPUT: FOUR-RAY PROPAGATION MODEL

ANT K:100.00 D:10000. D2 5000. F 100.0   TRGET HT FROM 0. TO 250. BY 10.
WAVELENGTH 1.760 POLARIZATION H   EPSILON L 15.000 EPSILON R 15.000 SIG L 0.005 SIG R 0.305
REFL

TRGT HT	RT	F 20LOG(F)	V(1)	MAG(E1)	RHO(1)	PHI(1)	V(2)	MAG(E2)	V(3)	MAG(E3)	RHO(2)	PHI(2)	V(4)	MAG(E4)
0.0	0.00	-56.42	-1.231	0.17	0.99	-179.988	-2.46	0.09	-1.231	0.17	0.99	-179.998	-2.46	0.09
10.0	0.19	-18.50	-1.108	0.19	0.99	-179.988	-2.34	0.09	-1.354	0.16	0.99	-179.987	-2.58	0.08
20.0	0.29	-10.78	-0.985	0.21	0.99	-179.988	-2.22	0.10	-1.477	0.15	0.99	-179.986	-2.71	0.08
30.0	0.26	-11.77	-0.862	0.23	0.99	-179.988	-2.09	0.11	-1.600	0.13	0.99	-179.985	-2.83	0.08
40.0	0.14	-16.86	-0.739	0.25	0.99	-179.988	-1.97	0.11	-1.723	0.13	0.99	-179.984	-2.95	0.07
50.0	0.21	-13.67	-0.615	0.28	0.99	-179.988	-1.85	0.12	-1.846	0.12	0.98	-179.983	-3.08	0.07
60.0	0.35	-9.02	-0.492	0.31	0.99	-179.988	-1.72	0.13	-1.969	0.11	0.98	-179.982	-3.20	0.07
70.0	0.39	-8.98	-0.369	0.35	0.99	-179.988	-1.60	0.14	-2.093	0.10	0.98	-179.980	-3.32	0.07
80.0	0.38	-9.34	-0.246	0.39	0.99	-179.988	-1.48	0.15	-2.216	0.10	0.98	-179.979	-3.45	0.06
90.0	0.38	-8.39	-0.123	0.44	0.99	-179.988	-1.35	0.16	-2.339	0.09	0.98	-179.978	-3.57	0.06
100.0	0.55	-5.22	0.0	0.50	0.99	-179.988	-1.23	0.17	-2.462	0.09	0.98	-179.977	-3.69	0.06
110.0	0.66	-3.65	0.123	0.57	0.99	-179.988	-1.11	0.19	-2.585	0.08	0.98	-179.976	-3.82	0.06
120.0	0.67	-3.46	0.246	0.64	0.99	-179.988	-0.98	0.20	-2.708	0.08	0.98	-179.975	-3.94	0.06
130.0	0.75	-2.48	0.369	0.72	0.99	-179.988	-0.86	0.22	-2.831	0.08	0.98	-179.973	-4.06	0.05
140.0	0.96	-0.39	0.492	0.80	0.99	-179.988	-0.74	0.25	-2.954	0.07	0.97	-179.972	-4.19	0.05
150.0	1.11	0.94	0.615	0.89	0.99	-179.988	-0.62	0.27	-3.077	0.07	0.97	-179.971	-4.31	0.05
160.0	1.18	1.44	0.739	0.97	0.99	-179.988	-0.49	0.31	-3.200	0.07	0.97	-179.970	-4.43	0.05
170.0	1.31	2.33	0.862	1.05	0.99	-179.988	-0.37	0.34	-3.323	0.07	0.97	-179.969	-4.55	0.05
180.0	1.51	3.60	0.985	1.12	0.99	-179.988	-0.25	0.39	-3.447	0.06	0.97	-179.968	-4.68	0.05
190.0	1.62	4.20	1.108	1.16	0.99	-179.988	-0.12	0.44	-3.570	0.06	0.97	-179.967	-4.80	0.04
200.0	1.62	4.21	1.231	1.17	0.99	-179.988	0.0	0.49	-3.693	0.06	0.97	-179.965	-4.92	0.04
210.0	1.66	4.41	1.354	1.15	0.99	-179.988	0.12	0.56	-3.816	0.06	0.97	-179.964	-5.05	0.04
220.0	1.65	4.37	1.477	1.09	0.99	-179.988	0.25	0.63	-3.939	0.06	0.97	-179.963	-5.17	0.04
230.0	1.85	3.25	1.600	1.01	0.99	-179.987	0.37	0.71	-4.062	0.05	0.97	-179.962	-5.29	0.04
240.0	1.15	1.24	1.723	0.93	0.99	-179.987	0.49	0.79	-4.185	0.05	0.96	-179.961	-5.42	0.04
250.0	0.84	-1.48	1.846	0.88	0.99	-179.987	0.62	0.88	-4.308	0.05	0.96	-179.960	-5.54	0.04

APPENDIX B

THE SMOOTH SPHERICAL-EARTH MODEL FOR THE INTERFERENCE REGION

This model implements in IBM FORTRAN IV ANSI the computation of propagation in the interference region over a smooth earth as described in KERR (1951), pp. 112-122.

For a specified radar wavelength, transmitting antenna height, and earth reflection coefficient, the program described here computes the pattern propagation factor for a sequence of target heights at a specified target range. Refraction is taken into account by specifying the earth-radius factor K; the true radius is taken as 6373 km. All parameters and variables are designated by the symbols used in that reference unless specified otherwise; the input and output quantities are as follows:

Input	Output
Target range (km) RNG	Table with the following columns:
Transmitter antenna height (m) Z1	Target Height
Earth radius factor AK	Pattern Propagation Factor F
Wavelength (cm) WAVE	F
Reflection coefficient	20 log F
Magnitude RHO	40 log F
Phase PHAZ	Grazing angle
Target height (m)	Distances
Starting height Z2S	R_1 transmitter to specular point
Ending height Z2E	R_2 target to specular point
Incremental step DZ2	
	Divergence factor
	ΔR path difference between direct and reflected waves
	First-Fresnel-Zone size
	S-MAJ semimajor axis
	S-MIN semiminor axis of the first Fresnel zone

69

Note that the output contains a number of geometrical quantities that are useful in evaluating the model predictions. For example, knowing the path difference ΔR, one can locate the boundary of the interference region, $\Delta R = \lambda/8$. The dimensions of the first Fresnel zone are calculated approximately by constructing a plane tangent to the earth at the specular point and calculating the dimensions of the semimajor and semiminor axes of the Fresnel ellipse on this tangent plane (see KERR, 1951, p. 415, Eqs. (31)-(33)).

This computation was programmed by Gerald McCaffrey; a copy of the program listings and a sample output, which includes a list of input parameters, follow this description. The sample output is plotted for $\lambda = 3.3$ cm in Fig. 6.7.

PROGRAM LISTINGS: SPHERICAL-EARTH MODEL, INTERFERENCE REGION

PROGRAMMED BY GERALD McCAFFREY

```
        DATA PI/3.14159/
        DATA RAD/57.2957795/
        DATA RADIUS/6373.0/
C
C       READ INPUTS, FROM INPUT FORM
C
        WRITE(6,10)
10      FORMAT(' INPUT TRAN HT,WAVELENGTH,EARTH RAD FACTOR,RHO AND PHASE')
        READ(5,*) Z1,WAVE,AK,RHO,PHAZ
        PZ1=Z1
C
C       CONVERT PHAZ TO RADIANS
C
        RPHZ=PHAZ/RAD
C
C       CALCULATE AE = THE EFFECTIVE EARTH RADIUS
C
        AE=RADIUS*AK
C
C       GET RANGE AND TARGET LOOPS SETUP
C
        WRITE(6,204)
204     FORMAT(' INPUT RANGE LOOP : RNGS,RNGE,DRNG')
        READ(5,*) RNGS,RNGE,DRNG
        WRITE(6,203)
203     FORMAT(' INPUT TARGET HEIGHT LOOP ;Z2ST,Z2E,DZ2')
        READ(5,*) Z2ST,Z2E,DZ2
        Z2S=Z2ST-DZ2
C
C       LOOP ON RANGE
C
        RNG=RNGS-DRNG
200     RNG=RNG+DRNG
        IF(RNG.GT.RNGE) GO TO 1000
        IC=0
        IC1=0
C
C       LOOP ON TARGET HEIGHT
C
        Z2S=Z2ST-DZ2
250     Z2S=Z2S+DZ2
        IF(Z2S.GT.Z2E) GO TO 200
        Z2=Z2S
        PZ2=Z2
```

71

```
C      CHECK THAT Z1.GE.Z2
C
       Z1=PZ1

       IF(Z1.GE.Z2) GO TO 20
C
C      IF NOT SWITCH Z1 AND Z2
C
       SAVE=Z1
       Z1=Z2
       Z2=SAVE
C
20     IC=IC+1
       IC1=IC1+1
C
C      CALCULATE R2 - DISTANCE TARGET TO REFLECTION (KM)
C
       A=AE*((Z1+Z2)/1000.0)
       B=(RNG/2.0)**2
       P=2.0/SQRT(3.0)*SQRT(A+B)
       ANG=ARCOS((Z2-Z1)*2*AE*RNG/(1000.0*P**3))
       R2=RNG/2.0+P*COS((ANG+PI)/3.0)
       R1=RNG-R2
       PR1=R1
       PR2=R2
       IF(PZ1.GE.PZ2) GO TO 25
       SAVE=PR1
       PR1=PR2
       PR2=SAVE
25     S1=R1/SQRT(2*AE*Z1/1000.0)
       S2=R2/SQRT(2*AE*Z2/1000.0)
       S=RNG/(SQRT(2*AE*Z1/1000.0)+SQRT(2*AE*Z2/1000.0))
       IF(S1.LT.1.AND.S2.LT.1.AND.S.LT.1) GO TO 30
       F=0
       F20=0
       F40=0
       X=0
       R1=0
       R2=0
       GO TO 39
30     T=SQRT(Z2/Z1)
       D1=4*S2*T*S1**2
       D2=S*(1-S1**2)*(1+T)
       D3=1+D1/D2
       D=1/SQRT(D3)
       X1=((1-S1**2)+T**2*(1-S2**2))/(1+T**2)
       X2=(Z1+Z2)/(1000.0*RNG)
       X3=X1*X2
```

```
          X=ATAN(X3)
          XDEG=X*RAD
          DR1=2*Z1*Z2/(10*RNG)
          DR2=(1-S1**2)*(1-S2**2)
          DR=DR1*DR2
          F1=1+RHO**2*D**2
          F2=2*RHO*D*COS((2*PI*DR/WAVE)+RPHZ)
          F=SQRT(F1+F2)

          F20=20*ALOG10(F)
          F40=40*ALOG10(F)
          Z1P=Z1-R1**2/(2*AE)
          Z2P=Z2-R2**2/(2*AE)
          CG=1+2*DR/WAVE
          CH=1+(Z1P+Z2P)**2/(10*WAVE*RNG)
          CI=SQRT(10*WAVE*RNG)
          CJ=1+2*Z1P*(Z1P+Z2P)/(10*WAVE*RNG)
          XO=RNG/2*CJ/CH
          IF(PZ2.GT.PZ1) XO=RNG-XO
          XC=RNG/2*SQRT(CG)/CH
          YC=CI/2*SQRT(CG/CH)
39        IF(IC.GT.1) GO TO 40
          WRITE(8,8999)
8999      FORMAT(50X,'PROP1(12/11/78 VERSION)')
          WRITE(8,9000) RNG,WAVE
9000      FORMAT('1',5X,'RANGE= ',F4.1,' KM',70X,'WAVELENGTH= ',F5.1,' CM')
          WRITE(8,9001) PZ1
9001      FORMAT(5X,'TRANSMITTER HEIGHT= ',F5.1,' M',57X,'REFLECTION COEFFIC
         1IENT')
          WRITE(8,9002) AK,RHO
9002      FORMAT(5X,'EARTH RADIUS FACTOR= ',F5.2,58X,'MAGNITUDE= ',F5.3)
          WRITE(8,9003) PHAZ
9003      FORMAT(89X,'PHASE= ',F6.1,/)
          WRITE(8,9004)
9004      FORMAT(2X,'TARGET HEIGHT',4X,'PATTERN PROPAGATION FACTOR',3X,'GRAZ
         1ING',8X,'R1',7X,'R2',7X,'DIV',5X,'DELTA-R',6X,'FIRST FRESNEL ZONE
         2')
          WRITE(8,9005)
9005      FORMAT(7X,'(M)',10X,'F',5X,'20LOG(F)',2X,'40LOG(F)',2X'ANGLE (DEG)
         1',5X,'(KM)',5X,'(KM)',5X,'FACTOR',5X,'(CM)',2X,'CENTER(KM)',1X,
         2'S-MAJ(KM)',2X,'S-MINOR(M)')
40        WRITE(8,9006) PZ2,F,F20,F40,XDEG,PR1,PR2,D,DR,XO,XC,YC
9006      FORMAT(F10.2,F13.2,F10.2,F10.2,F10.2,F13.2,F9.2,F11.3,F9.2,F9.3,F9
         1.3,F13.2)
          WRITE(1,45) RNG,PZ2,F20,F40
45        FORMAT(4F12.4)
          IF(IC1.EQ.4) WRITE(8,9007)
9007      FORMAT(' ')
          IF(IC1.EQ.4) IC1=0
          GO TO 250
1000      RETURN
          END
```

SAMPLE OUTPUT: SPHERICAL-EARTH MODEL, INTERFERENCE REGION

PROP1(12/11/78 VERSION)

RANGE= 30.0 KM
TRANSMITTER HEIGHT= 30.0 M
EARTH RADIUS FACTOR= 1.33

WAVELENGTH= 3.3 CM
REFLECTION COEFFICIENT=
MAGNITUDE= 0.700
PHASE= 180.0

TARGET HEIGHT (M)	PATTERN PROPAGATION FACTOR			GRAZING ANGLE (DEG)	E1 (KM)	P2 (KM)	DIV FACTOR	DELTA-R (CM)	FIRST FRESNEL ZONE		
	F	20LOG(F)	40LOS(F)						CENTER(KM)	S-MAJ(KM)	S-MINOR(M)
10.00	0.72	-2.82	-5.64	0.02	19.70	10.30	0.431	0.18	19.630	6.042	10.25
20.00	1.10	0.86	1.71	0.04	16.97	13.03	0.554	0.87	17.188	5.263	10.36
30.00	1.41	2.98	5.95	0.06	15.00	15.00	0.623	1.87	15.000	4.730	10.68
40.00	0.60	-4.42	-8.85	0.08	13.48	16.56	0.672	3.08	13.218	4.272	10.92
50.00	1.35	2.58	5.16	0.10	12.16	17.84	0.712	4.44	11.753	3.863	11.07
60.00	1.00	0.02	0.05	0.12	11.08	18.92	0.745	5.91	10.546	3.499	11.12
70.00	1.18	1.42	2.83	0.14	10.15	19.85	0.778	7.47	9.582	3.178	11.10
80.00	1.12	1.02	2.04	0.15	9.35	20.65	0.798	9.10	8.659	2.897	11.08
90.00	1.20	1.61	3.22	0.17	8.65	21.35	0.819	10.78	7.984	2.650	10.95
100.00	1.03	0.22	0.44	0.19	8.34	21.96	0.838	12.51	7.371	2.433	10.84
110.00	1.36	2.78	5.56	0.20	7.49	22.51	0.854	14.27	6.842	2.241	10.72
120.00	0.74	-2.61	-5.22	0.22	7.01	22.99	0.868	16.06	6.380	2.072	10.58
130.00	1.57	3.90	7.81	0.24	6.58	23.42	0.881	17.88	5.975	1.922	10.85
140.00	0.39	-8.11	-16.22	0.26	6.19	23.81	0.891	19.72	5.616	1.789	10.31
150.00	1.62	4.18	8.37	0.27	5.85	24.15	0.901	21.58	5.297	1.669	10.17
160.00	0.64	-3.96	-7.72	0.29	5.53	24.47	0.910	23.45	5.013	1.562	10.03
170.00	1.40	2.94	5.87	0.31	5.25	24.75	0.917	25.38	4.754	1.466	9.89
180.00	1.23	1.62	3.23	0.33	4.99	25.01	0.924	27.24	4.522	1.379	9.76
190.00	0.89	-1.06	-2.12	0.35	4.75	25.25	0.930	29.15	4.310	1.299	9.62
200.00	1.60	4.06	8.11	0.36	4.53	25.47	0.936	31.06	4.117	1.227	9.50

APPENDIX C

BIBLIOGRAPHY: RADAR PROPAGATION AT LOW ALTITUDES

This bibliography covers the subject of radio and microwave propagation,
VHF through X-band, near the surface of the earth. References are indexed
under the headings of Books, Journal Articles, and Technical Reports and cross-
referenced in a Subject Index. Although many of the references cited here
deal with one-way propagation, the results are directly applicable to the
radar (two-way) case as explained in Sec. 2. We assembled this bibliography
as we surveyed the literature on the effects of propagation on ground-radar
performance against low-flying aircraft. All listed references were examined
and found relevant to this general subject; the references judged most useful
are marked with an asterisk. In striving for completeness we have included
some references of marginal value, but all are worthy of examination if their
title or their listing in the Subject Index suggests that they may be of inter-
est. References in the text of this report and in the Subject Index are
labeled by the last names of authors and the year of publication. The Author
Index contains the complete reference information. Major headings in the
Subject Index are listed alphabetically below.

1. Diffraction Effects
2. Frequency Bands
3. Height-Gain Measurements
4. Microwave Links
5. Mobile Communication
6. Models for Loss Computation
7. Ocean, Propagation Over
8. Reflection Effects
9. Refraction Effects and Rain Attenuation
10. Review Articles and Reports
11. Spherical Earth, Propagation Over
12. Tracking Accuracy, Propagation Effects on

75

BOOK INDEX

BARTON (1975)

D.K. Barton, "Radars, Volume 4: Radar Resolution and Multipath Effects," Artech House, Inc., Dedham, Mass.

BECKMANN & SPIZZICHINO (1963)

P. Beckmann and A. Spizzichino, "The Scattering of Electromagnetic Waves from Rough Surfaces," Pergammon Press, Oxford. (Distributed by MacMillan Co., New York)

BORN & WOLF (1959)

M. Born and E. Wolf, "Principals of Optics," Pergammon Press, London.

BRODHAGE & HORMUTH (1977)

H. Brodhage and W. Hormuth, "Planning and Engineering of Radio Relay Links," Eighth Edition, Heyden & Son Ltd., London.

BURROWS & ATTWOOD (1949)

C.R. Burrows and S.S. Attwood, "Radio Wave Propagation," Academic Press, New York.

FINK (1957)

D.G. Fink, "Television Engineering Handbook," (Chapter 14, Wave Propagation, Radiation and Absorption) McGraw-Hill, New York.

BOOK INDEX

JAKES (1974)

W.C. Jakes, Editor, "Microwave Mobile Communications," (Chapter 2 by D.O. Rendink, Large-Scale Variations of the Average Signal) John Wiley and Sons, New York.

KERR (1951)

D.E. Kerr, Editor, "The Propagation of Short Radio Waves," Vol. 13, Radiation Laboratory Series, McGraw-Hill, New York.

LANGER (1962)

R.E. Langer, Editor, "Electromagnetic Waves," Proceedings of a Symposium Conducted by the Mathematics Research Center, University of Wisconsin, Madison, 10-12 April 1961, University of Wisconsin Press, Madison

LIVINGSTON (1970)

D.C. Livingston, "The Physics of Microwave Propagation," Prentice-Hall Inc., Englewood Cliffs, N.J.

MEEKS (1976)

M.L. Meeks, Editor, "Methods of Experimental Physics," volume 12B, Radio Telescopes, Academic Press, New York.

BOOK INDEX

REED & RUSSELL (1953)

H.R. Reed and C.M. Russell, "Ultra
High Frequency Propagation," John
Wiley and Sons, New York.

JOURNAL-ARTICLE INDEX

Adams (1978)

B.W.P. Adams, "An Empirical Routine for Estimating Reflection Loss in Military Radio Paths in the VHF and UHF Bands," in "International Conference on Antennas and Propagation, Part 2, Propagation," IEE Conference Publication No. 169, London.

* Anderson, Trolese
& Weisbrod (1960)

L.J. Anderson, L.G. Trolese, "Simplified Method of Computing Knife-Edge Diffraction in the Shadow Region," in "Electromagnetic Wave Propagation," edited by M. Desirant and J. Michiels, Academic Press, New York.

Anderson (1963)

E.W. Anderson, "The SHF Radio Link Comes of Age," Point to Point Communication 7, 4-15

Bachynski (1959)

M.P. Bachynski, "Microwave Propagation Over Rough Surfaces," RCA Rev. 20, 308-335

Bachynski (1960)

M.P. Bachynski, "Propagation at Oblique Incidence Over Cylindrical Obstacles," J. Res. Nat. Bur. Stand. Sect. D, 64D, 311-315

Bachynski & Kingsmill (1962)

M.P. Bachynski & M.G. Kingsmill, "Effect of Obstacle Profile on Knife-Edge Diffraction," IRE Trans. Antennas Propag. AP-10, 201-205

Bachynski (1963)

M.P. Bachynski, "Scale-Model Investigations of Electromagnetic Wave Propagation Over Natural Obstacles," RCA Rev. 24, 105-144

Barrick (1971)

D.E. Barrick, "Theory of HF and UHF Propagation across the Rough Sea," Radio Sci. 6, 517-533

Barsis, Barghausen, & Kirby (1963)

A.P. Barsis, A.F. Barghausen, & R.S. Kirby, "Studies of Within-the-Horizon Propagation at 9300 Mc," IEEE Trans. Antennas Propag. AP-11, 24-38

JOURNAL-ARTICLE INDEX

Barton (1974)

D. K. Barton, "Low-Angle Radar Tracking," Proc. IEEE 62, 687-704

* Barton (1977)

D. K. Barton, "Radar Multipath Theory and Experimental Data," IEE International Conference Radar-77 London, October 1977.

Barton (1979a)

D.K. Barton, "Multipath Fluctuation Effects in Track-While-Scan Radar," IEEE Trans. Aerospace Electr. Sys. AES-15: 754-764

Barton (1979b)

D.K. Barton, "Low-Altitude Tracking Over Rough Surfaces I: Theoretical Predictions," in EASCON '79 Record, IEEE Electronics and Aerospace Systems Convention, Arlington, Virginia, IEEE Publication. 79CH 1476-1 AES

Beard et al. (1956)

C.I. Beard, I. Katz, and L.M. Spetner "Phenomological Vector Model of Microwave Reflection from the Ocean," IRE Antennas Propag. AP-4, 162-167

JOURNAL-ARTICLE INDEX

* Beard (1961)

C.I. Beard, "Coherent and In-coherent Scattering of Micro-waves from the Ocean," _IRE Trans_. _AP-9_, 470-83

Beard (1967)

C.I. Beard, "Behavior of Non-Rayleigh Statistics of Micro-wave Forward Scatter from a Random Water Surface," _IEEE Trans_. _Antennas Propag_. _AP-15_, 649-657

Beckmann (1965)

P. Beckmann, "Shadowing of Random Rough Surfaces," _IEEE Trans_. _Antennas Propag_. _AP-13_, 384-388

Beckmann (1973)

P. Beckmann, "Scattering by Non-Gaussian Surfaces," _IEEE Trans_. _Antennas Propag_. _AP-21_, 169-175

Black & Reudink (1972)

D.M. Black & D.O. Reudink, "Some Characteristics of Mobile Radio Propagation at 836 MHz in the Philadelphia Area," _IEEE Trans_. _Vehicular Tech_. _VT-21_, 45-51

Blue (1980)

M.D. Blue, "Permittivity of Ice and Water at Millimeter Wavelengths," *J. Geophys. Res.* **85**, 1101-1106

Boyd & Deavenport (1973)

M.L. Boyd & R.L. Deavenport, "Forward and Specular Scattering from a Rough Surface," *J. Acoust. Soc. Am.* **53**, 791-801

Brockelman & Hagfors (1966)

R.A. Brockelman & T. Hagfors, "Note on the Effect of Shadowing on the Backscattering of Waves from a Random Rough Surface," *IEEE Trans. Antennas Propag.* **AP-14**, 621-629

Brown & Epstein & Peterson (1948)

G.H. Brown & J. Epstein & D.W. Peterson, "Comparative Propagation Measurements; Television Transmitters at 67.25, 288,510 and 910 Megacycles," *RCA Rev. IX*, 177-201

Bullington (1950a)

K. Bullington, "Propagation of UHF and SHF Waves Beyond the Horizon," *Proc. IRE* **38**, 1221-1222

JOURNAL-ARTICLE INDEX

Bullington (1950b)

K. Bullington, "Radio Propagation Variations at VHF and UHF," Proc. IRE 38, 27-32

* Bullington (1954)

K. Bullington, "Reflection Coefficients of Irregular Terrain," Proc. IRE 42, 1258-62

Bullington (1957)

K. Bullington, "Radio Propagation Fundamentals," Bell Syst. Tech. J. 36, 593-626

Clarke & Hendry (1964)

R.H. Clarke & G.O. Hendry, "Prediction and Measurement of the Coherent and Incoherent Power Reflected from a Rough Surface," IEEE Trans. Antennas Propag. AP-12, 353-363

Cornwell & Landcaster (1979)

P.E. Cornwell & J. Landcaster, "Low-Altitude Tracking Over Rough Surfaces II: Experimental and Model Comparisons," IEEE Trans. Aerospace Electr. Sys., in EASCON '79 Record, IEEE Record, IEEE Electronics and Aerospace Systems Convention, Arlington, Virginia, IEEE Publication 79CH 1476-1 AES.

JOURNAL-ARTICLE INDEX

Crawford & Jakes (1952)   A.B. Crawford & W.C. Jakes, "Selection Fading of Microwaves," Bell Syst. Tech. J. 31, 68-90

Crysdale (1955)   J.H. Crysdale, "Correspondence: Comments on Dickson et al," (1953) Proc. IRE 43, 627-628

Cumming (1952)   W.A. Cumming, "The Dielectric Properties of Ice and Snow at 3.2 Centimeters," J. Appl. Phys. 23, 768-773

Dadson (1979)   C.E. Dadson, "Radio Network and Radio Link Surveys Derived by Computer from a Terrain Data Base," in AGARD Conference Proceedings No. 269, North Atlantic Treaty Organization, Advisory Group for Aerospace Research and Development

Davies (1975)   H.G. Davies, "Scattering of Acoustic Point-Source Fields by Random Surfaces," J. Acoust. Soc. Am. 57, 1403-1408

JOURNAL-ARTICLE INDEX

* Day & Trolese (1950) J.P. Day and L.G. Trolese, "Propagation of Short Radio Waves Over Dessert Terrain," Proc. IRE 38, 165-175

DeAssis (1971) M. S. DeAssis, "A Simplified Solution to the Problem of Multiple Diffraction over Rounded Obstacles," IEEE Trans. Antennas Propag. AP-19, 292-295

Delaney & Meeks (1979) J.R. Delaney & M.L. Meeks, "Prediction of Radar Coverage Against Very Low Altitude Aircraft," in AGARD Conference Proceedings No. 269, North Atlantic Treaty Organization, Advisory Group for Aerospace Research and Development.

DeLange (1951) O.E. DeLange, "Propagation Studies at Microwave Frequencies by Means of Very Short Pulses," Bell Sys. Tech. J. 31: 91-103

JOURNAL-ARTICLE INDEX

DeLorenzo & Cassedy (1966)

J.D. DeLorenzo & E.S. Cassedy, "A Study of the Mechanism of Sea Surface Scattering," IEEE Trans. Antennas and Propag. AP-14: 611-620

* Deygout (1966)

J. Deygout, "Multiple Knife-Edge Diffraction of Microwaves," IEEE Trans. Antennas Propag. AP-14, 480-489

Dickson et al. (1953)

F.H. Dickson, J.J. Egli, J.W. Gerbstreit, & G.S. Wickizer, "Large Reductions of VHF Transmission Loss and Fading by the Presence of a Mountain Obstacle in Beyond-Line-of-Sight Paths," Proc. IRE 41, 967-969

* Domb & Pryce (1946)

C. Domb & M.H.L. Pryce, "The Calculation of Field Strengths Over a Spherical Earth," Inst. Electrical Engineers J. 94, 325-339

Domb (1953)

C. Domb, "Tables of Functions Occurring in the Diffraction of Electromagnetic Waves by the Earth," Adv. Phys., 5, 96-102

JOURNAL-ARTICLE INDEX

Dougherty & Maloney (1964)   H.T. Dougherty & L.J. Maloney, "Application of Diffractions by Convex Surfaces," Radio Sci. 68D, 239-250

Durkee (1948)   A.L. Durkee, "Results of Microwave Propagation Tests on a 40-Mile Overland Path," Proc. IRE 36, 197-205

* Edwards & Durkin (1969)   R. Edwards & J. Durkin, "Computer Prediction of Service Areas for VHF Mobile Radio Networks," Proc. IEE 116: 1493-1500

Egli (1957)   J.J. Egli, "Radio Propagation Above 40 MC Over Irregular Terrain," Proc. IRE 45, 1383-1391

* Epstein & Peterson (1953)   J. Epstein & D.W. Peterson, "An Experimental Study of Wave Propagation at 850 MC," Proc. IRE 41, 595-611

JOURNAL-ARTICLE INDEX

* Evans (1965)

S. Evans, "Dielectric Proper-
ties of Ice and Snow -- a Re-
view," J. Glaciology, 5, 773-
792

Forbes (1968)

E.J. Forbes, "Planning 13-GHz
TV Relay Systems," Trans. IEEE
Broadcasting BC-14, 19-24

* Ford & Oliver (1946)

L.H. Ford & R. Oliver, "An Ex-
perimental Investigation of the
Reflection and Absorption of
Radiation of 9 cm Wavelength,"
Proc. Phys. Soc. London, 58,
265-280

Fung & Ulaby (1978)

A.K. Fung & F.T. Ulaby, "A
Scatter Model for Leafy Veg-
etation," IEEE Trans. Geo-
science Electr., GE-16, 281-
286

Furutsu (1966)

K. Furutsu, "A Statistical
Theory of Ridge Diffraction,"
Radio Sci. 1, 74-98

JOURNAL-ARTICLE INDEX

Glenn (1968)

A.B. Glenn, "Fading from Irregular Surfaces for Line-of-Sight Communications," _IEEE Trans. on Aerospace & Electronics Syst._ AES-4, 149-163

Gough (1962)

M.W. Gough, "Propagation Influences in Microwave Link Operation," _J. British IRE_ 24, 53-72

Hacking (1968)

K. Hacking, "Optical Diffraction Experiments Simulating Propagation Over Hills at UHF," _Inst. Elect. Eng., London, Conf._ 48, 58-65

* Hacking (1970)

K. Hacking, "UHF Propagation Over Rounded Hills," _Proc. IEE_ 117, 499-511

Hamlin & Gordon (1948)

E.W. Hamlin & W.E. Gordon, "Comparison of Calculated and Measured Phase Difference at 3.2 Centimeters Wavelength," _Proc. IRE_ 36, 1218-23

JOURNAL-ARTICLE INDEX

Hayes, Lammers, et al. (1979)   D.T. Hayes, V.H. Lammers, R.A. Marr, and J.J. McNally "Millimeter Propagation Measurements Over Snow," in EASCON '79 Record, IEEE Electronics and Aerospace Systems Convention, Arlington, Virginia, IEEE Publication 79CH 1476-1 AES.

Head (1960)   H.T. Head, "The Influence of Trees on Television Field Strengths at Ultra-High Frequencies," Proc. IRE 48, 1016-1020

Hearson (1967)   L.T. Hearson, "Unusual Propagation Factors in Point-to-Point Microwave System Performance," IEEE Trans. on Communication Technology COM-15, 615-625

Hortenbach (1970)   J. Hortenbach, "Multiple Ground Reflection Effects on Fading Behavior of VHF/UHF Satellite Transmissions," IEEE Trans. Antennas Propag. AP-18, 836-838

91

JOURNAL-ARTICLE INDEX

Hufford (1952)

G.A. Hufford, "An Integral Equation Approach to the Problems of Wave Propagation Over an Irregular Surface," Quarterly J. Applied Math 9, 391-404

Jakes & Reudink (1967)

W.C. Jakes, Jr. & D.O. Reudink, "Comparison of Mobile Radio Transmission at UHF and X-Band," IEEE Trans. on Vehicular Tech. VT-16, 10-14

Josephson & Blomquist (1958)

B. Josephson & A. Blomquist, "The Influence of Moisture in the Ground, Temperature and Terrain on Ground Wave Propagation in the VHF-Band," IRE Trans. Antennas Propag., AP-6, 169-172

Klein & Swift (1977)

L.A. Klein & C.T. Swift, "An Improved Model for the Dielectric Constant of Sea Water at Microwave Frequencies," IEEE Trans. Antennas Propag., AP-25, 104-111

JOURNAL-ARTICLE INDEX

LaGrone & Straiton (1949)
A.H. LaGrone & A.W. Straiton, "The Effect of Antenna Size and Height Above Ground on Pointing for Maximum Signal," Proc. IRE 37, 1438-42

LaGrone (1960)
A.H. LaGrone, "Forecasting Television Service Fields," Proc. IRE 48, 1009-1016

LaGrone & Chapman (1961)
A.H. LaGrone & C.W. Chapman, "Some Propagation Characteristics of High UHF Signals in the Immediate Vicinity of Trees," IRE Trans. Ant. Prop. 9, 487-491

LaGrone, Martin & Chapman (1963)
A.H. LaGrone, P.E. Martin, and C.W. Chapman, "Height Gain Measurements at VHF & UHF Behind a Grove of Trees," IEEE Trans. on Broadcasting BC-9, 37-53

Legg (1965)
A.J. Legg, "Propagation Measurements at 11 Gc/s Over a 35 Near-Optical Path Involving Diffraction at Two Obstacles," Electron. Lett. 1, 285-286

JOURNAL-ARTICLE INDEX

Lelliott & Thurlow (1965)

S.R. Lelliott & E.W. Thurlow, "Path Testing for Microwave Radio-Relay Links," Post Office Electrical Engineers Journal 58, 26-31

Linlor (1980)

W.I. Linlor, "Permittivity and Attenuation of Wet Snow Between 4 and 12 GHz," J. Appl. Phys., 51, 2811-2816

Littlewood (1967)

C.A. Littlewood, "Microwave Path Testing," Telephony 172, 16-18

Lonquet-Higgins (1960a)

M.S. Lonquet-Higgins, "Reflection and Refraction at a Random Moving Surface. I. Pattern and Paths of Specular Points," J. Opt. Soc. Am. 50, 838-844

Lonquet-Higgins (1960b)

M.S. Lonquet-Higgins, "Reflection and Refraction at a Random Moving Surface. II. Number of Specular Points in a Gaussian Surface," J. Opt. Soc. Am. 50, 845-850

JOURNAL-ARTICLE INDEX

Lopez (1970)

A.R. Lopez, "Ray-Diffraction Method for Handling Complex Incident Fields," *IEEE Trans. Antennas Propag.*, AP-18, 821-823

Lynch & Wagner (1970)

P.J. Lynch & R.J. Wagner, "Rough Surface Scattering: Shadowing, Multiple Scattering and Energy Conservation," *J. Math. Phys.* 11, 3032-3042

McGarty (1976)

T.P. McGarty, "Antenna Performance in the Presence of Diffuse Multipath," *IEEE Trans. Aerospace and Electr. Sys.* AES-12, 42-54

McGavin & Maloney (1959)

R.E. McGavin & L.J. Maloney, "Study at 1,046 Megacycles per Second of the Reflection Coefficient of Irregular Terrain at Grazing," *J. Res. Nat. Bur. Stand. D. Radio Propagation* 63D, 235-248

McMahon (1974)   J.H. McMahon, "Interference
                                  and Propagation Formulas and
                                  Tables Used in the Federal
                                  Communications Commission
                                  Spectrum Management Task Force
                                  Land Mobile Frequency Assign-
                                  ment Model," IEEE Trans. on
                                  Vehic. Tech. VT-23, 129-134

McPetrie & Ford (1964)   J.S. McPetrie & L.H. Ford,
                                  "Some Experiments on the Prop-
                                  agation Over Land of Radiation
                                  of 9.2-Wavelength, Especially
                                  on the Effect of Obstacles,"
                                  J. IEE 93, 531-538

Millington (1960)   G. Millington, "A Note on
                                  Diffraction Round a Sphere or
                                  Cylinder," Marconi Rec. 23,
                                  170-182

* Millington, Hewitt & Immirzi   G. Millington, R. Hewitt, and
  (1962)   F.S. Immirzi, "Double Knife-
                                  Edge Diffraction in Field-
                                  Strength Predictions," Proc.
                                  IEE 109C, 419-429

JOURNAL-ARTICLE INDEX

* Mrstik & Smith (1978)

A.V. Mrstik and P.G. Smith, "Multipath Limitations on Low-Angle Radar Tracking," _IEEE Trans. Aerospace Electr. Sys._ AES-14, 85-102

Neugebauer & Bachynski (1958)

H.E.J. Neugebauer & M.P. Bachynski, "Diffraction by Smooth Cylindrical Mountains," _Proc. IRE_ 46, 1619-1627

Neugebauer & Bachynski (1960)

H.E.J. Neugebauer & M.P. Bachynski, "Diffraction by Smooth Conical Obstacles," _J. Res. Nat. Bur. Stand. Sec. D_, 64D, 317-329

Norton (1941)

K.A. Norton, "The Calculation of Ground-Wave Field Intensity Over a Finitely Conducting Spherical Earth," _Proc. IRE_ 29, 623-639

JOURNAL-ARTICLE INDEX

Ott (1971)

R.H. Ott, "An Alternative Integral Equation for Propagation Over Irregular Terrain, 2," Radio Sci. 6, 429-435

Ott, Vogler, and Hufford (1979)

R.H. Ott, L.E. Vogler, and G.A. Hufford, "Ground-Wave Propagation Over Irregular Inhomogeneous Terrain: Comparisons of Calculations and Measurements," IEEE Trans. Antennas Propag. AP-27, 284-286

* Oxehufwud (1959)

A. Oxehufwud, "Tests Conducted Over Highly Reflective Terrain at 4,000, 6,000, and 11,000 Megacycles," Trans. American IEE 78, 265-270

Palmer (1979)

F.H. Palmer, "VHF/UHF Path-Loss Calculations Using Terrain Profiles Deduced from a Digitial Topographic Data Base," in AGARD Conference Proceedings No. 269 North Atlantic Organization Advisory Group for Aerospace Research and Development, September 1979

JOURNAL-ARTICLE INDEX

Rocco & Smith (1949)

M.D. Rocco & J.B. Smith, "Diffraction of High-Frequency Radio Waves Around the Earth," Proc. IRE 37, 1195-1203

Ruze, Sheftman, & Cahlander (1966)

J. Ruze, F.I. Sheftman, & D.A. Cahlander, "Radar Ground-Clutter Shields," Proc. IEEE 54, 1171-1183

Saxton (1950)

J.A. Saxton, "Reflection Co-efficient of Snow and Ice at V.H.F.," Wireless Engineer., 27, 17-25

Saxton & Lane (1955)

J.A. Saxton & J.A. Lane, "V.H.F. and U.H.F. Reception," Wireless World 61, 229-232

Schelleng & Burrows & Ferrell (1933)

J.C. Schelleng & C.R. Burrows & E.B. Ferrell, "Ultra-Short-Wave Propagation," Proc. IRE 21, 427-463

Selvidge (1941)

H. Selvidge, "Diffraction Measurements at Ultra-High Frequencies," Proc. IRE 29, 10-16

JOURNAL-ARTICLE INDEX

* Sherwood & Ginzton (1955)

E.M. Sherwood & E.L. Ginzton, "Reflection Coefficients of Irregular Terrain at 10 cm," Proc. IRE 43, 877-878

Shkarofsky, Neugebauer & Bachynski (1958)

I.P. Shkarofsky, H.E.J. Neugebauer, & M.P. Bachynski, "Effects of Mountains with Smooth Crests on Wave Propagation," IRE Trans. Antennas Propag. AP-6, 341-348

* Smith (1967)

B.G. Smith, "Geometrical Shadowing of Random Rough Surfaces," IEEE Trans. Antennas Propag. AP-15, 668-671

Smith & Mrstik (1979)

P.G. Smith & A.V. Mrstik, "Multipath Tracking Errors in Elevation-Scanning and Monopulse Radars," IEEE Trans. Aerospace Electr. Sys. AES-15, 765-776

Stogryn (1971)

A. Stogryn, "Equations for Calculating the Dielectric Constant of Saline Water," IEEE Trans. Microwave Theory Techs., MT-19, 733-735

Straiton (1952)

A.W. Straiton, "Microwave Radio Reflection from Ground and Water Surfaces," IRE Trans. Antennas Propag. PGAP-4, 37-45

Straiton & Tolbert (1956)

A.W. Straiton & C.W. Tolbert, "Measurement and Analysis of Instantaneous Radio Height-Gain Curves at 8.6 Millimeters Over Rough Surfaces," IRE Trans. Antennas Propag. AP-4 346-351

Stutzman, Colliver & Crawford (1979)

W.L. Stutzman, F.W. Colliver, & H.S. Crawford, "Microwave Transmission Measurements for Estimation of the Weight of Standing Pine Trees," IEEE Trans. Antennas Propag. AP-27: 22-26

JOURNAL-ARTICLE INDEX

Tomlinson & Straiton (1959)

H.T. Tomlinson & A.W. Straiton, "Analysis of 3-cm Radio Height-Gain Curves Taken Over Rough Terrain," IRE Trans. Antennas Propag. AP-7, 405-413

Twersky (1957)

V. Twersky, "On Scattering and Reflection of Electromagnetic Waves by Rough Surfaces," IRE Trans. Antennas Propag. AP-5: 81-90

Van der Pol & Bremmer (1937)

D. Van der Pol & H. Bremmer, "The Diffraction of Electro-magnetic Waves...Round a Finitely Conducting Sphere....," Philos. Mag. Part 1, 24, 141-176, Part 2, 24, 825-864

Vogler (1964)

L.E. Vogler, "Calculation of Ground Wave Attenuation in the Far Diffraction Region," Radio Sci. 68-D, 819-826

* Wagner (1967)

R.J. Wagner, "Shadowing of Randomly Rough Surfaces," J. Acoust. Soc. Am. 41, 138-146

JOURNAL-ARTICLE INDEX

* Wait & Conda (1959)

J.R. Wait & A.M. Conda, "Diffraction of Electromagnetic Waves by Smooth Obstacles for Grazing Angles," _J. Res. Nat. Bur. Stand._ 63-D, 181-197

Watt & Maxwell (1960)

A.D. Watt & E.L. Maxwell, "Measured Electrical Properties of Snow and Glacial Ice," _J. Res. Nat. Bur. Stand. Sect. D_, 64D, 357-363

Wetzel (1977)

L.B. Wetzel, "A Model for Sea Backscatter Intermittency at Extreme Grazing Angles," _Radio Sci._ 12, 749-756

* White (1974)

W.D. White, "Low-Angle Radar Tracking in the Presence of Multipath," _IEEE Trans. Aerospace Electr. Sys._ AES-10, 835-852

Young (1952)

W.R. Young, "Comparison of Mobile Radio Transmission at 150, 450, 900, and 3700 Mc," _Bell Syst. Tech. J._ 31, 1068-1085

Barton (R1976)   D.K. Barton, "Forward Scatter
                                        at Low Grazing Angles," in
                                        "DARPA Low-Angle Tracking
                                        Symposium," Defense Advanced
                                        Research Projects Agency,
                                        General Research Corp., Santa
                                        Barbara, California, B020494

Bean, Horn & Ozanich, Jr. (R1960)   B.R. Bean, J.D. Horn, & A.M.
                                        Ozanich, Jr., "Climatic Charts
                                        and Data of the Radio Refrac-
                                        tive Index for the United
                                        States and the World, Mono-
                                        graph 22," United States De-
                                        partment of Commerce, National
                                        Bureau of Standards, Washington,
                                        D.C.

Beckmann (R1967)   P. Beckmann, "Scattering from
                                        Rough Surfaces and Finite Dis-
                                        tances Between Transmitter and
                                        Receiver," Geo-Astrophysics
                                        Laboratory, Boeing Scientific
                                        Research Laboratories, Seattle,
                                        Washington, AD 666 593

Capon (R1976)

J. Capon, "Multipath Parameter Computations for the MLS Simulation Computer Program," Final Report FAA-RD-76-55, Massachusetts Institute of Technology, Lincoln Laboratory, Lexington, Massachusetts, AD-A024350

Carlson (R1967)

N.L. Carlson, "Dielectric Constant of Vegetation at 8.5 GHz," Technical Report 1903-5, Ohio State University, Electro Science Laboratory, Columbus, Ohio

* Crane (R1977)

R.K. Crane, "Microwave Scattering Parameters for New England Rain," Final Technical Report 426, Massachusetts Institute of Technology, Lincoln Laboratory, Lexington, Massachusetts, AD-647798

Electromagnetic Compatibility Analysis Center † (R1978)

"ECAC Capabilities for Terrain-Dependent Line-of-Sight and Radio Coverage Analysis," (no report number given) Electromagnetic Compatability Research Center, Annapolis, Maryland

---

† No author given

TECHNICAL-REPORT INDEX

Haakinson, Violette & Hufford (R1980)

E.J. Haakinson, E.J. Violette, and G.A. Hufford, "Propagation Effects on an Intervisibility Measurement System," NITA-Report-80-35, Department of Commerce, Institute for Tele-communication Sciences, Boulder, Colo. (February 1980)

Kalinin (R1958)

A.N. Kalinin, "Approximate Methods of Calculating the Field Strength of Ultra Short Waves Taking Into Account the Influence of Local Terrain," Translation 6005 National Bureau of Standards, Boulder, Colo. (September 1958)

Kammerer & Richer (R1964)

J.E. Kammerer & K.A. Richer, "4.4 mm Near-Earth Antenna Multipath Pointing Errors," Memorandum Report No. 1559, Ballistic Research Laborato-ries, Aberdeen Proving Ground, Maryland, AD-443211

LeBay (R1977)

P.M. LeBay, III, "Low Frequency Radar Systems Should Replace High Frequency Radar Systems on the Battlefield to Optimize the Army's Ground Surveillance Radar Capability," Masters-Degree Thesis, Student at the U.S. Army Command and General Staff College, Fort Leavenworth, Kansas, AD-A043739

* Longley & Rice (R1968)

A.G. Longley and P.L. Rice, "Prediction of Tropospheric Radio Transmission Loss over Irregular Terrain -- a Computer Method, 1968," Department of Commerce, ESSD Research Laboratories Report ERL 79-ITS 67, U.S. Government Printing Office. Modification to this computer model published as an Appendix to Department of Commerce, Office of Telecommunications Report 78-144, (April 1978)

TECHNICAL-REPORT INDEX

Longley & Reasoner (R1970)   A.G. Longley & R.K. Reasoner,
                              "Comparison of Propagation
                              Measurements with Predicted
                              Values in the 20 to 10,000 MHz
                              Range, Technical Report ERL
                              148-ITS 97, Institute for Tele-
                              communications Sciences,
                              Boulder, Colorado, AD-703579

Longley & Hufford (R1975)   A.G. Longley & G.A. Hufford,
                              "Sensor Path Loss Measurements
                              Analysis and Comparison with
                              Propagation Models," OT Report
                              75-74, Institute for Telecom-
                              munications Sciences, Office
                              of Telecommunications, U.S.
                              Department of Commerce,
                              Boulder, Colorado, PB-247638

Longley (R1976)   A.G. Longley, "Location Vari-
                              ability of Transmission Loss
                              -- Land Mobile and Broadcast
                              Systems," OT-Report 76-87,
                              Institute for Telecommunica-
                              tions Sciences, Office of Tele-
                              communications, U.S. Department
                              of Commerce, Boulder, Colorado,
                              PB-254472

TECHNICAL-REPORT INDEX

Longley & Reasoner & Fuller
(R1977)

A.G. Longley, R.K. Reasoner, and V.L. Fuller, "Measured and Predicted Long-Term Distributions of Trophospheric Transmision Loss," Report OT/TRER 16, Institute for Telecommunications Sciences, Boulder, Colorado, COM 75-112 05/2ST

Longley (R1978)

A.G. Longley, "Radio Propagation in Urban Areas," Report 78-144 U.S. Department of Commerce, Office of Telecommunications, Boulder, Colorado, PB-281932

McCue (R1978)

J.J.G. McCue, "The Evaporation Duct and Its Implications for Low-Altitude Propagation at Kwajalein," Technical Note 1978-6, Lincoln Laboratory, Massachusetts Institute of Technology, Massachusetts (11 May 1979)   AD-A057117

TEHNICAL-REPORT INDEX

McGarty (R1974)

T.P. McGarty, "Models of Multipath Propagation Effects in a Ground-to-Air Surveillance System," Technical Note 1974-7, Lincoln Laboratory, Massachusetts Institute of Technology, Lexington, Massachusetts, AD-777241

Moene (R1966)

A. Moene, "The Monthly Frequency of Occurrence of Meteorological Conditions Favourable for Duct-Propagation of Radar-Waves in the NW-Europe 1965," Interm Report E-79, Norwegian Defence Research Establishment, Kjeller - Norway

O'Dowd, Dyer & Tuley (R1978)

W.M. O'Dowd, Jr., F.B. Dyer, and M.T. Tuley, "Effects of the Ocean Surfaces on the Forward Scattering of Radar Signals at Low Incidence Angles," Final Report No. 1873, Georgia Institute of Technology, Engineering Experiment Station, Atlanta, Georgia

TECHNICAL-REPORT INDEX

Peake & Oliver (R1971)

W.H. Peake, & T.L. Oliver, "The Response of Terrestrial Surfaces at Microwave Frequencies," Technical Report AFAL-TR-70-301, Air Force Avionics Laboratory, Air Force Systems Command, Wright-Patterson Air Force Base, Ohio

* Rice, Longley, Norton, & Barsis (R1967)

P.L. Rice, A.G. Longley, K.A. Norton, and A.P. Barsis, "Transmission Loss Predictions for Trophospheric Communication Circuits," Technical Note 101, Volumes I & II, Institute for Telecommunication Sciences and Aeronomy, Boulder, Colorado, AD-687820 & AD-687721

Samson (R1975)

C.A. Samson, "Refractivity Gradients in the Northern Hemisphere," OTR 75-59, U.S. Department of Commerce, Office of Telecommunications, Institute for Telecommunication Sciences, Boulder, Colorado, AD-A009503

TECHNICAL-REPORT INDEX

* Samson (R1976)

C.A. Samson, "Refractivity and Rainfall Data for Radio Systems Engineering," Department of Commerce, Office of Telecommunications Report OTR 76-105, (September 1976).

Schlussler (R1973)

H. Schlussler, "UHF Propagation Path Loss Measurements at Low Grazing Angles," Technical Report ECOM-4106, U.S. Army Electronics Command, Fort Monmouth, New Jersey, AD-910305

Schouten (R1971)

A. Schouten, "Attenuation Effect of Foliage Upon Radar-Frequency Propagation -- Results of a Trial at Pershore (UK), Technical Memorandum STC TM-310, Shape Technical Centre, The Hague, AD-888431

* Segal & Barrington (R1977)

B. Segal & R.E. Barrington, "The Radio Climatology of Canada: Tropospheric Refractivity Atlas for Canada," Department of Communications (Canada), Communications Research Centre Report No. 1315-E (December 1977).

TECHNICAL-REPORT INDEX

Sun (R1979)

D.F. Sun, "Experimental Meas-
urements of Ground Reflection
Elevation Multipath Character-
istics and Its Effects on a
Small Aperture Elevation track-
ing Radar," Technical Note
1979-21, Massachusetts Insti-
tute of Technology, Lincoln
Laboratory, Lexington,
Massachusetts, AD-A0977915

Wang (R1979)

J.R. Wang, "The Dielectric
Properties of Soil-Water Mix-
tures at Microwave Frequencies,"
Technical Memorandum 80597,
NASA Goddard Space Flight Cen-
ter, Greenbelt, Maryland

Zehner & Tuley (R1979)

S.P. Zehner & M.T. Tuley,
"Development and Validation
of Multipath and Clutter
Models for TAC ZINGER in Low
Altitude Scenarios," Final
Report, Engineering Experiment
Station, Georgia Institute of
Technology, Atlanta, Georgia

SUBJECT INDEX

1. **Diffraction effects**

   cylinders, calculation of diffraction by

       Bachynski (1960)

       Capon (R1976)

       Dougherty & Maloney (1964)

       Millington (1960)

      * Pryce (1953)

       Rice (1954)

      * Wait & Conda (1959)

   cylinder, measurement of diffraction by

       Bachynski (1960)

   experimental studies of

       Bullington (1950b)

     * Day & Trolese (1950)

       Delaney & Meeks (1979)

       Dougherty & Maloney (1964)

     * Epstein & Peterson (1953)

       Lagrone, Martin & Chapman (1963)

       Lelliott & Thurlow (1965)

       Littlewood (1967)

       McPetrie & Ford (1964)

       Neugebauer & Bachynski (1958)

       Neugebauer & Bachynski (1960)

       Oxehufwud (1959)

       Rocco & Smith (1949)

       Schlussler (R1973)

       Selvidge (1941)

SUBJECT INDEX

SUBJECT INDEX

SUBJECT INDEX

SUBJECT INDEX

9. <u>Refraction effects & rain attenuation</u>

   Bean, Horn, & Ozanich, Jr. (R1960)

  * Crane (R1977)

   Crawford & Jakes (1952)

   DeLange (1951)

   Durkee (1948)

   Hamlin & Gordon (1948)

   Legg (1965)

   McCue (R1978)

   Moene (R1966)

   Nottarp (1967)

   Rocco & Smith (1949)

   Samson (R1975)

  * Samson (R1976)

  * Segal & Barrington (R1977)

   Tomlinson & Straiton (1959)

10. <u>Review articles & reports</u>

   Bachynski (1959)

   Barton (1974)

  * Barton (1977)

   Bullington (1957)

   Egli (1953)

   Epstein & Peterson (1953)

   Forbes (1968)

   Glenn (1968)

SUBJECT INDEX

Review articles & reports (continued)

Gough (1962)

Kalinin (K1958)

LaGrone (1960)

Longley & Reasoner (R1970)

Longley, Reasoner & Fuller (R1971)

McGarty (1976)

* Mrstik & Smith (1978)

* Rice, Longley, Norton, & Barsis (R1967)

Sexton & Lane (1955)

Schelleng, Burrows, & Ferrell (1933)

11. Spherical earth, propagation over

Domb (1953)

* Domb & Pryce (1946)

Norton (1941)

Norton, Rice, & Vogler (1955)

* Pryce (1953)

Van der Pol & Bremmer (1937)

Vogler (1964)

12. Tracking accuracy, propagation effects on

Armstrong, Cornwell, & Greene (R1974)

Barton (R1976)

* Barton (1977)

Barton (1979a)

Barton (1979b)

SUBJECT INDEX

131

REPORT DOCUMENTATION PAGE		READ INSTRUCTIONS BEFORE COMPLETING FORM
1. REPORT NUMBER ESD-TR-81-98	2. GOVT ACCESSION NO. AD-A103 773	3. RECIPIENT'S CATALOG NUMBER
4. TITLE (and Subtitle) Radar Propagation at Low Altitudes: A Review and Bibliography		5. TYPE OF REPORT & PERIOD COVERED Technical Report 6. PERFORMING ORG. REPORT NUMBER Technical Report 580
7. AUTHOR(s) M. Littleton Meeks		8. CONTRACT OR GRANT NUMBER(s) F19628-80-C-0002
9. PERFORMING ORGANIZATION NAME AND ADDRESS Lincoln Laboratory, M.I.T. P.O. Box 73 Lexington, MA 02173		10. PROGRAM ELEMENT, PROJECT, TASK AREA & WORK UNIT NUMBERS Program Element No. 62301E Project No. 1E10 ARPA Order No. 3724
11. CONTROLLING OFFICE NAME AND ADDRESS Defense Advanced Research Projects Agency 1400 Wilson Boulevard Arlington, VA 22209		12. REPORT DATE 31 June 1981
		13. NUMBER OF PAGES 140
14. MONITORING AGENCY NAME & ADDRESS (if different from Controlling Office) Electronic Systems Division Hanscom AFB Bedford, MA 01731		15. SECURITY CLASS. (of this report) Unclassified
		15a. DECLASSIFICATION DOWNGRADING SCHEDULE

16. DISTRIBUTION STATEMENT (of this Report)

Approved for public release; distribution unlimited.

17. DISTRIBUTION STATEMENT (of the abstract entered in Block 20, if different from Report)

18. SUPPLEMENTARY NOTES

None

19. KEY WORDS (Continue on reverse side if necessary and identify by block number)

electromagnetic wave propagation
ground-based radar

low-flying aircraft
low-altitude propagation

20. ABSTRACT (Continue on reverse side if necessary and identify by block number)

This report reviews the subject of electromagnetic wave propagation near the earth's surface as it relates to the detection of low-flying aircraft by ground-based radars. Separate sections describe how current knowledge of the three fundamental physical phenomena — refraction, reflection, and diffraction — is applied to the problems of low-altitude propagation. Simple models incorporating these phenomena are discussed: (1) propagation over a plane with arbitrary reflection coefficient, (2) propagation over a knife-edge on a plane, and (3) propagation over a smooth, spherical earth. Computer programs for models (2) and (3) are given in the Appendices. We include a bibliography of the literature on which this report is based: books, journal articles, and technical reports. References are listed alphabetically by first author, and subject indices are given for major subject headings.

DD FORM 1473 EDITION OF 1 NOV 65 IS OBSOLETE
1 JAN 73

207650